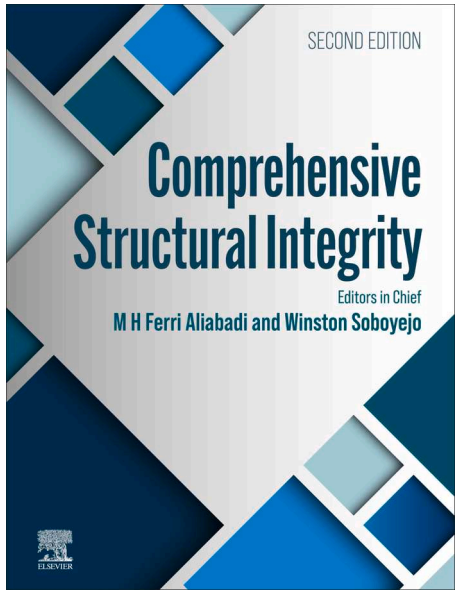

Oyewole, Oluwaseun K., Adeniji, Sharafadeen A., Oyewole, Deborah O., Koech, Richard, Oyelade, Omolara V., Cromwell, Jaya, Olanrewaju, Yusuf, Bello, Abdulhakeem and Soboyejo, Winston O. (2023) Fatigue of Flexible and Stretchable Electronic Structures. In: Aliabadi, Ferri M H and Soboyejo, Winston (eds.) *Comprehensive Structural Integrity, 2nd Edition,* vol. 4, pp. 266–285. Oxford: Elsevier.

http://dx.doi.org/10.1016/B978-0-12-822944-6.00035-9

Fatigue of Flexible and Stretchable Electronic Structures

Oluwaseun K Oyewole, Department of Mechanical Engineering, Worcester Polytechnic Institute, Worcester, MA, United States and Materials Science and Engineering Program, Department of Mechanical Engineering, Worcester Polytechnic Institute, Worcester, MA, United States
Sharafadeen A Adeniji, Department Theoretical and Applied Physics, African University of Science and Technology, Abuja, Federal Capital Territory, Nigeria
Deborah O Oyewole, Department of Mechanical Engineering, Worcester Polytechnic Institute, Worcester, MA, United States and Materials Science and Engineering Program, Department of Mechanical Engineering, Worcester Polytechnic Institute, Worcester, MA, United States
Richard Koech, Department of Mechanical Engineering, Worcester Polytechnic Institute, Worcester, MA, United States and Department Materials Science and Engineering, African University of Science and Technology, Abuja, Federal Capital Territory, Nigeria
Omolara V Oyelade, Department Theoretical and Applied Physics, African University of Science and Technology, Abuja, Federal Capital Territory, Nigeria
Jaya Cromwell, Department of Mechanical Engineering, Worcester Polytechnic Institute, Worcester, MA, United States
Yusuf Olanrewaju
Abdulhakeem Bello, Department Theoretical and Applied Physics, African University of Science and Technology, Abuja, Federal Capital Territory, Nigeria
Winston O Soboyejo, Department of Mechanical Engineering, Worcester Polytechnic Institute, Worcester, MA, United States and Materials Science and Engineering Program, Department of Mechanical Engineering, Worcester Polytechnic Institute, Worcester, MA, United States

Abstract

Reliability of electronic systems that are used for applications where flexibility and stretchability are required are becoming necessary in this modern world. Since these flexible and stretchable electronic structures are designed to undergo stress-induced deformation during service condition, it is importance to understand their fatigue behavior. In this article, the underlying fatigue behavior of the flexible and stretchable structures is presented. The theories of failure phenomena that occur during fabrication and deformations of these structures are elucidated. The detailed fatigue test and analysis of the structures are then presented before exploring the failure mechanisms and their effects on optoelectronic properties.

Nomenclature

FSE Flexible and Stretchable
ITO Indium Tin Oxide
P3HT:PCBM poly(3-hexylthiophene):phenyl-C61-butyric acid methyl ester
PDMS Polydimethylsiloxane
PEDOT:PSS Poly(3,4-ethylenedioxythiophene):polystyrene sulfonate
PeLEDs Perovskite Light Emitting Devices
PEN Poly (ethylene 2, 6-naphthalene dicarboxylate)
PET Polyethylene terephthalate
PU Polyurethane
PVA Polyvinylachohol
SOSCs Stretchable Organic Solar Cells

Key Points

- Fatigue of flexible and stretchable solar cells is explored.
- The mechanics of deformation of stretchable structures are highlighted.
- Root cause failure of flexible and stretchable solar cell structures under service conditions are elucidated.
- Design and fatigue testing procedures for flexible and stretchable solar cell structures are provided.
- The failure mechanisms are studied along with their effects on optoelectronic properties of stretchable solar cells.

Introduction

There has been increasing interest in the development of efficient, low-cost, and robust flexible and stretchable electronic (FSE) systems (Baran *et al.*, 2020; Forrest, 2004). These electronic systems are subjected to different modes of deformation such as folding, twisting, wrinkling, bending, and stretching during handling and while in operation (Kim *et al.*, 2019; Yi *et al.*, 2018). They can also experience induced stresses due to thermal expansion mismatch between any of the adjacent thin films. The FSE structures have found applications in solar cells (Asare *et al.*, 2015, 2017; Kaltenbrunner *et al.*, 2012; Kim *et al.*, 2008; Lipomi *et al.*, 2011, 2012; Oyewole *et al.*, 2015c, 2020; Sekitani *et al.*, 2008), light emitting devices(Bade *et al.*, 2017; Oyewole *et al.*, 2015d,b; Sekitani *et al.*, 2008, 2009), soft robotics (Kim *et al.*, 2019), portable and wearable electronics (Kan and Lam, 2021), bio-integrated health monitoring devices (Liu *et al.*, 2017) and many other electronic systems (Bade *et al.*, 2017; Lacour *et al.*, 2005, 2006; Sekitani *et al.*, 2009).

Mechanical robustness of these electronic structures depends on their ability to withstand repeated stretching (Lipomi *et al.*, 2011, 2012; Oyewole *et al.*, 2015a; Oyewole, 2015; Oyewole *et al.*, 2020), bending (Asare *et al.*, 2015; Kim and Rogers, 2008) or twisting (Li *et al.*, 2005; Lipomi *et al.*, 2011; Oyewole *et al.*, 2020) without inducing failure in their layered constituents or interfaces. It is, therefore, of interest to understand the underlying reliability failure of these FSE structures under repeated (cyclic) deformations in a way that provide insights into effects fatigue failure on optoelectronic performance. The understand of the reliability of these structures is very important under various forms of repeated mechanical distortions that are usually encountered during service conditions (Liu *et al.*, 2017; Su *et al.*, 2012; Wu, 2019).

FSE structures are made up of multilayered films that are fabricated on flexible or stretchable substrates. The level flexibility and stretchability of these electronic structures depend on the compliancy of the substrates used. Among the substrates used for flexible/stretchable electronic structures include: polyethylene terephthalate (PET); poly (ethylene 2, 6-naphthalene dicarboxylate) (PEN); polyurethane (PU); polyvinylachohol (PVA), and polydimethylsiloxane (PDMS). While stretchable electronic structures can withstand high level of cyclic stretching, bending and twisting before initiation failure in the layered structures, flexible electronic devices can withstand cyclic bending before any noticeable failure (Asare *et al.*, 2015; Oyewole *et al.*, 2020). The lifetime of these devices under deformation depends on the extent of induced stresses/strains in layered constituents.

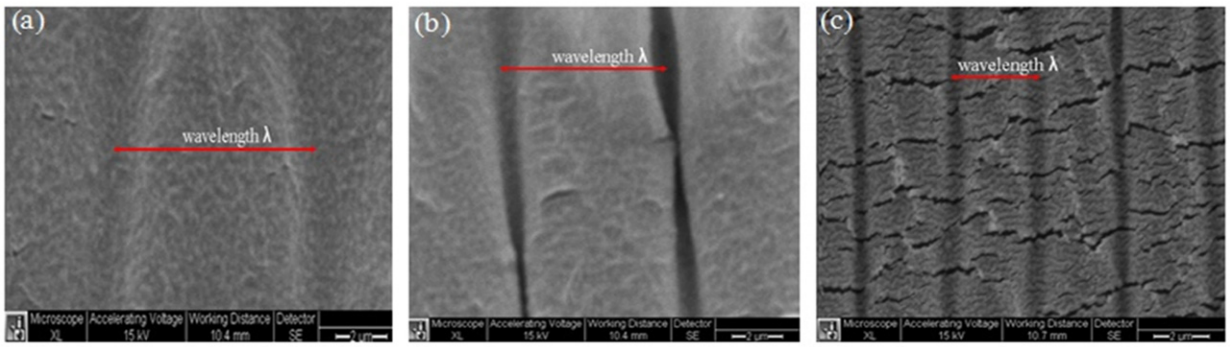

Fig. 1 Micro-wrinkled profiles for different pre-strain values: (a) 18%, (b) 36% and (c) 70%. Reproduced from Oyewole, O.K., Yu, D., Du, J., *et al.*, 2015a. Micro-wrinkling and delamination-induced buckling of stretchable electronic structures. Journal of Applied Physics 117(23), with permission of AIP Publishing.

Several innovative design principles and structural modifications have been proposed to develop robust stretchable structures. These include: use of polymeric substrates, engineering of the materials (Kim *et al.*, 2019), tailoring the geometries, and blending brittle materials with elastic polymeric compounds. Geometrical patterning and structural design strategies such as buckling and design of wavy configurations, use of fractal structures, percolating networks, and kirigami approaches are other techniques that have been used to enhance flexibility and stretchability (Fan *et al.*, 2014; Kim *et al.*, 2008; Shyu *et al.*, 2015). The overall concept is to design systems that can absorb mechanical strains with self-healing capabilities after some form of mechanical deformation.

Generally, the layered constituents of flexible/stretchable electronic structures are intrinsically not stretchable or bendable to a significant small radius (Heidari *et al.*, 2017; Saleh *et al.*, 2021). Therefore, numerous efforts have been made to disperse such materials in layers that increase the overall deformability of the intrinsically elastic materials (Lee *et al.*, 2011a). The stretchability have also been improved by incorporating polymeric materials into the layers in a way that make them fully stretchable. In the case of stretchable solar cells, the layered structures have been made stretchable by buckling/wrinkling phenomena in films that are deposited after the stretching process (Dennler *et al.*, 2005; Lee *et al.*, 2011a; Lipomi *et al.*, 2011, 2012; Oyewole *et al.*, 2020; Sekitani *et al.*, 2008, 2009; Sun and Rogers, 2007). The stretching behavior of organic solar cells have been increased by Lipomi *et al.* (2011) while the failure mechanisms associated with deformation have been identified by Oyewole *et al.* (2020).

The understanding of fatigue behavior and failure of the emerging stretchable solar cells and light emitting devices that are made from organic and hybrid perovskite materials is very important for the design of robust structures that can last longer. In the case of stretchable organic solar cells, interfacial failure can also occur between the adjacent layers (Oyewole *et al.*, 2015d; Tong *et al.*, 2009; Yu *et al.*, 2014a). Failure can also occur by buckling-induced delamination/interfacial cracking, which can cause a lot of scattering of light that is meant for generation of excitons (Agyei-Tuffour *et al.*, 2017a; Oyewole, 2015). Such scattering can disrupt transportation of charges that can cause degradation in the optoelectronic properties of stretchable electronic devices (Oyewole *et al.*, 2020). There is, therefore, a need to develop a fundamental understanding of the adhesion/interfacial failure in layered structures of stretchable organic solar cells under fatigue. Hence, it is important to study the potential effects of cyclic loading on the optoelectronic properties of these stretchable organic electronic structures.

Several failure mechanisms have been identified in stretchable inorganic electronic structures under deformation. These include deformation and cracking mechanisms in metallic thin films deposited on stretchable substrates (Akogwu *et al.*, 2010; Bowden *et al.*, 1998, 1999; Lacour *et al.*, 2004, 2006; Midturi, 2010). In stretchable metallic thin films (such as stretchable gold), failure mechanisms are associated with the elastic-plastic deformation of nano-scale gold layers on poly(dimethyl-siloxane) substrates (Akogwu *et al.*, 2010; Akogwu *et al.*, 2010; Midturi, 2010). with occurrence of deformation-induced film buckling, wrinkling, cracking and delamination (Akogwu *et al.*, 2010; Midturi, 2010) as shown in **Fig. 1**(a)-(c). The mechanic models that predict some of these failure mechanisms in stretchable electronic structures have been proposed (Huang *et al.*, 2003; Jia *et al.*, 2011; Suo *et al.*, 2003; Tucker *et al.*, 2009). The onset of cracking in these structures occurred at relatively low strains. Furthermore, most of the metallic thin films (that were deposited using evaporation or e-beam techniques) have been found to experience significant residual stresses (Akogwu *et al.*, 2010; Evans and Hutchinson, 1995; Lacour *et al.*, 2006; Midturi, 2010) due to the thermal expansion mismatch between the films and the substrates.

In this article, the understanding of fatigue behavior of FSE structures that is needed for design and fabrication of reliable FSE systems such as flexible circuit systems, stretchable circuit boards, stretchable solar cells and stretchable light emitting devices. A combined experimental and theoretical approach is provided for studying the fatigue behavior and failure of FSE structures. Following the introduction in Section "Introduction", the mechanics of failure in FSE structures are presented in Section "Mechanics of Failure in Flexible/Stretchable Thin Films". The mechanics of wrinkling failure of FSE structures for small and finite deformations are shown before highlighting the 2D mechanics of one dimensional and checker mode of deformations. The mechanics of fracture in flexible and stretchable thin films are also presented in a way that discuss the possible delamination-induced buckling and interfacial cracking in FSE structures under deformation.

The overviews of the designs and fabrication of FSE structures are presented in Section "Root Cause of Failure of Stretchable Electronic Devices During Operation". These include the designs and typical fabrication procedures of stretchable organic solar cells and stretchable perovskite light emitting devices. Section "Design of Flexible/Stretchable Electronic Structures" presents the fatigue test and analysis for layered stretchable thin film structures that are deposited on polymeric substrates. The detailed fatigue failures in FSE structures are elucidated in Section "Fatigue Test and Analysis in Stretchable Electronic Structures" before exploring the underlying effects of the fatigue failure on optoelectronic properties of stretchable solar cells and stretchable light emitting devices in Section "Fatigue Failure in Flexible/Stretchable Electronic Devices". The summary and concluding remarks of the article are then presented in Section "Effects of Fatigue Failure on Stretchable Electronic Structures".

Mechanics of Failure in Flexible/Stretchable Thin Films

Most stretchable electronic structures are fabricated using wrinkling and delamination-induced buckled geometries that are caused by pre-stretch and thermal compressive residual stresses (Evans and Hutchinson, 1995; Mei and Huang, 2013; Watanabe, 2012; Watanabe *et al.*, 2002). The formation and deformation of wrinkles can initiate failure that can then result to delamination (Ebata *et al.*, 2012) of layered stretchable electronics structures. Under static or cyclic loading conditions, the nucleation and growth of cracks at surfaces can induce interfacial failure which lead to adhesive or cohesive failure.

In layered structures, buckles occur in the presence of interfacial voids, before and after the release of the pre-stretched or by merging of micro voids that lead to delamination (Ebata *et al.*, 2012). It also possible that clean room particles or particles from undissolved precursors are sandwiched between the deposited films (Tong *et al.*, 2009). Some bubbles can also generate interfacial voids/cracks that can lead to failure (Momodu *et al.*, 2014; Oyewole *et al.*, 2015d). The delamination of multilayer structures from the substrate can also be caused by residual stress. It is, therefore, important to explore some theory of failure in stretchable thin films. In this session, we present theoretical analysis for the interfacial failures based on buckling mechanics and establish the criteria for the failure modes.

Mechanics of 1D Wrinkling

Small deformation theory

The energy approach has been utilized to predict the buckling geometry of the thin film with 1D sinusoidal profile based on plane strain in small deformation theory (Huang *et al.*, 2015; Khang *et al.*, 2009). The total energy is minimized in the form of wrinkling with specific wavelength and amplitude (Genzer and Groenewold, 2006) In a bilayer system, a stiff thin film with thickness, h_f, Poisson ratio, ν_f, and elastic modulus, E_f, is attached to a pre-stretched thick compliant substrate with Young's modulus, E_s, and Poisson ratio, ν_s. The substrate is assumed to be much more compliant than the thin film and thus $E_s \ll E_f$. Upon release of pre-strain, ε_{pre}, the thin film wrinkles with wavelength λ_0 and amplitude A_0. The out-of-plane displacement of the wrinkle can be expressed as (Khang *et al.*, 2009).

$$w = A_0 \cos(kx_1) = A_0 \cos\left(\frac{2\pi x_1}{\lambda_0}\right) \tag{1}$$

where x_1 is the coordinate along the film length direction. The total energy per unit length of the film-substrate system consists of the membrane energy, U_m, bending energy, U_b, in the thin film, and the strain energy, U_s , in the substrate which is given as

$$U_{tot} = U_b + U_m + U_s = \frac{\pi^4 \overline{E}_f h_{fA_0^2}^3}{3\lambda_0^4} + \frac{1}{2}\overline{E}_f h_f \left(\frac{\pi^2 A_0^2}{\lambda_0^2} - \varepsilon_{pre}\right)^2 + \frac{\pi}{4\lambda_0}\overline{E}_s A_0^2 \tag{2}$$

where $\overline{E}_f = E_f/(1-\nu_f^2)$ and $\overline{E}_s = E_s/(1-\nu_s^2)$ are the plane strain moduli of the film and substrate, respectively.

Minimizing the total energy with respect to buckling amplitude and wavelength (such that $\partial U_{tot}/\partial A_0 = \partial U_{tot}/\partial \lambda_0 = 0$) gives the buckling wavelength λ_0 and amplitude A_0 as (Huang *et al.*, 2005).

$$\lambda_0 = 2\pi\left(\frac{\overline{E}_f}{3\overline{E}_s}\right)^{1/3}, A_0 = h_f\sqrt{\frac{\varepsilon_{pre}}{\varepsilon_c} - 1} \tag{3}$$

where $\varepsilon_c = 1/4/(3\overline{E}_s/\overline{E}_f)^{2/3}$ is the critical buckling strain. If the pre-strain applied to the substrate is smaller than ε_c, buckling does not occur. It has been shown that both the buckling wavelength and amplitude of the stretchable silicon thin film on polymeric substrate increased with the thickness of the film (Khang *et al.*, 2009). The membrane strain used in the small deformation buckling theory remains constant after buckling, $\varepsilon_m = -\varepsilon_c$, and the maximum bending strain $\varepsilon_b = 2\pi^2 A h_f/\lambda^2$ increases with the deformation of the system. When the film is much stiffer than the substrate ($E_f \gg E_s$), the membrane strain (i.e., the critical buckling strain) is negligibly small. Hence, the peak strain in the thin film is approximately given as

$$\varepsilon_{peak} \approx 2\sqrt{\varepsilon_{pre}\varepsilon_c} \tag{4}$$

Finite deformation theory

In the small deformation theory, buckling wavelength is independent of the pre-strain. When large strains are applied, the wavelength decreases with the pre-strain. A finite deformation theory has been developed to explain this phenomenon, using the energy method (Jiang *et al.*, 2007; Song *et al.*, 2008a,b). The buckling wavelength and amplitude are given as (Jiang *et al.*, 2007; Song *et al.*, 2008a,b).

$$\lambda = \frac{\lambda_0}{(1+\varepsilon_{pre})(1+\xi)^{1/a}}, \quad A = \frac{A_0}{\sqrt{1+\varepsilon_{pre}}(1+\xi)^{1/a}} \tag{5}$$

where λ_0 and A_0 are the wavelength and amplitude in Eq. (3) and $\xi = 5\varepsilon_{pre}(1+\varepsilon_{pre})/32$. The membrane strain is negligible for a very stiff thin film on a compliant substrate (Song *et al.*, 2008b). The thin film's peak strain can be calculated roughly as:

$$\varepsilon_{peak} \approx 2\sqrt{\varepsilon_{pre}\varepsilon_c}\frac{(1+\xi)^{1/3}}{\sqrt{1+\varepsilon_{pre}}} \tag{6}$$

When a wrinkling system is subjected to external strain $\varepsilon_{applied}$, the wavelength and amplitude become

$$\lambda = \frac{\lambda_0(1+\varepsilon_{applied})}{(1+\varepsilon_{pre})(1+\varepsilon_{applied}+\zeta)^{1/a}}, \quad A = \frac{h\sqrt{(\varepsilon_{pre}-\varepsilon_{applied})/\varepsilon_c - 1}}{\sqrt{1+\varepsilon_{pre}}(1+\varepsilon_{applied}+\xi)^{1/a}} \tag{7}$$

where $\zeta = 5(\varepsilon_{pre}-\varepsilon_{applied})(1+\varepsilon_{pre})/32$. The peak strain of the film is given as:

$$\varepsilon_{peak} = 2\sqrt{(\varepsilon_{pre}-\varepsilon_{applied})\varepsilon_c}\frac{(1+\varepsilon_{applied}+\xi)^{1/3}}{\sqrt{1+\varepsilon_{pre}}} \tag{8}$$

Mechanics of 2D Wrinkling

In 2D, strain mismatch in bilayer system of stiff thin films form wrinkles that are more complicated than the 1D sinusoidal patterns. Surface morphological patterns such as 1D sinusoidal wavy pattern, checkerboard pattern, and herringbone pattern are the most common (Song *et al.*, 2008a).

To investigate the wrinkling of stiff thin films on compliant substrates in two dimensions, a spectral approach has been used to show that when the pre-strain is above the critical buckling strain, the surface morphology reveals a checkerboard pattern, which evolves to a herringbone pattern as the pre-strain increases. A finite element model has also been used to investigate the energetics of 2D wrinkling, and it was found that the herringbone pattern has the lowest energy (Chen and Hutchinson, 2004).

Using energy method systematic investigation of the 1D, checkerboard and herringbone buckling modes for 2D wrinkling (Chattopadhyay, 2007; Song *et al.*, 2008a), analytical solutions for all three modes can be obtained for biaxial pre-strains ε_{11}^{pre} and ε_{22}^{pre}.

One dimensional mode

The out-of-plane displacement and buckling wavelength are the same as in 1D wrinkling mechanics (as given by Eq. (1) and (3)). The amplitude is denoted by

$$A = h_f\sqrt{\frac{\varepsilon_{11}^{pre} + \nu_f\varepsilon_{22}^{pre}}{1/4/(3\overline{E}_s/\overline{E}_f)^{2/3}} - 1} \tag{9}$$

For plane strain condition ($\varepsilon_{22}^{pre}=0$), the amplitude is the same as given in Eq. (3). In the case of equibiaxial pre-strains ($\varepsilon_{11}^{pre}=\varepsilon_{22}^{pre}=\varepsilon_{pre}$), amplitude A becomes

$$A = h_f\sqrt{\frac{\varepsilon_{pre}}{\varepsilon_{1D}^c} - 1} \tag{10}$$

where $\varepsilon_{1D}^c = \left(3\overline{E}_s/\overline{E}_f\right)^{\frac{2}{3}}/\left(1+\nu_f\right)$ is the critical strain for 1D buckling mode.

Checker mode

In the case of Checker mode, the Checker out-of-plane displacement is given by

$$w = A\cos(k_1x_1)cos(k_2x_2) \tag{11}$$

For equibiaxial pre-strains ($\varepsilon_{11}^{pre}=\varepsilon_{22}^{pre}=\varepsilon_{pre}$), the wave number and amplitude are.

$k_1 = k_2 = \dfrac{1}{\sqrt{2}\frac{1}{h_f}\left(\frac{3\overline{E}_s}{\overline{E}_f}\right)^{1/3}}$,

$$A = h_f\sqrt{\frac{1}{(3-\nu_f)(1+\nu_f)}\left(\frac{\varepsilon_{pre}}{\varepsilon_{checkerboard}^c} - 1\right)} \tag{12}$$

where $\varepsilon_{checkerboard}^c = \left(3\overline{E}_s/\overline{E}_f\right)^{\frac{2}{3}}/\left(1+\nu_f\right)$ is the critical strain for checkerboard buckling mode. Analytical solutions have also been obtained for general biaxial prestrains $\varepsilon_{11}^{pre} \neq \varepsilon_{22}^{pre}$.

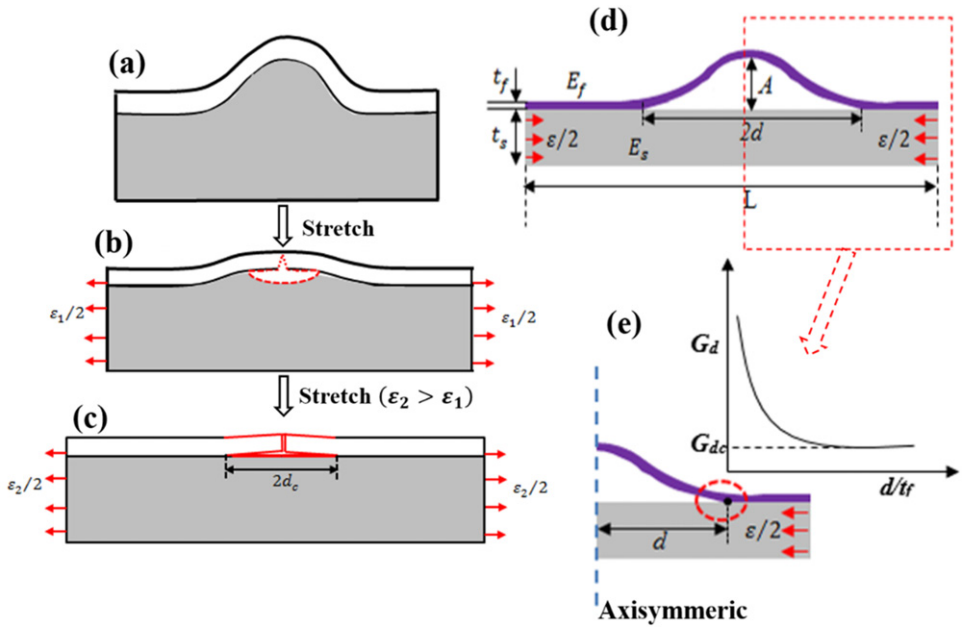

Fig. 2 Schematics of failure in stretchable solar cell structures: (a) A simple bi-layered structure of wrinkled structure, (b) interfacial delamination and initiation of cracking in film upon stretching, (c)delamination-induced cracking upon further stretching, (d)bi-layered model of interfacial crack driving force, and (e) axisymmetric model the crack driving force. Reproduced from Oyewole, Oluwaseun, Oyewole, Deborah, Oyelade, Omolara, *et al.*, 2020. Failure of stretchable organic solar cells under monotonic and cyclic loading. Macromolecular Materials and Engineering 305 (11), 2000369, with the permission of Wiley Publishing.

Herringbone mode

In the case of Herringbone mode, the out-of-plane displacement is given by

$$w = A\cos\{k_1[x_1 + B\cos(k_2 x_2)]\} \tag{13}$$

where $k_1 = 2\pi/\lambda_1$, $k_2 = 2\pi/\lambda_2$, A is the out-of-plane amplitude, B is the in-plane jog amplitude. In 2D buckling, the herringbone mode produces the least amount of energy, making it the most energy-efficient mode. The fundamental principle is that, in comparison to the other modes, the herringbone mode reduces thin film membrane energy while marginally increasing thin film bending and substrate strain energy.

Thin Film Fracture Mechanics

Basic knowledge of fracture mechanics is essential for the understanding fatigue failure in stretchable thin films. Fracture occurs in layered materials when the stress that is applied is greater than the critical stress. During service, residual stress can initiate cracks in the stretchable films and along the interface between the films and the substrates. Upon several cyclic deformations, the crack can also grow in the substrate if the substrate is not compliant enough. There can also be cohesive or adhesive separation between the films and the substrate. In the case of interfacial crack growth between the films and substrates, fracture can be referred to as breaking of bonds that cause interfacial adhesion between the two layers.

Stress-induced fracture in the films can be due to thermal mismatch between the film and the substrate. In most stretchable layered structures, thin films are deposited onto pre-stretched substrate. When the film is deposited at a temperature that is different from the substrate, the total stress on the film has two components: the residual stress due temperature mismatch and mechanical stress due to the pre-stretched substrate (Akogwu *et al.*, 2010). Therefore, stretchable thin films are generally wrinkled or buckled. The wrinkled stretchable films exhibit no interfacial delamination between the films and substrates while buckling in the buckled stretchable thin films is driven by induced-delamination of the films on elastomeric substrates.

The initial work on the understanding of mechanics of thin films on elastomeric substrates have shown that when compressive stresses in the films exceed the critical buckling stress, the film can buckle away from the substrate, for a given interfacial crack length. Periodic buckling patterns have been observed in free-standing bi-layered thin films of graphene that are generated by liquid-phase processing (Mao *et al.*, 2011), while non-sinusoidal surface profiles of buckled gold thin films have also been observed on elastomeric substrates due to different strengths in tension and compression that are resulted from grain micro-structure of the film (Fei *et al.*, 2009).

The understanding of the level of strain-to-wrinkling/buckling is very important in the development of layered stretchable electronic structures. Analytical solution has been used to predict critical strain for the onset of wrinkling of thin films on pre-strained polymeric substrates with small and large pre-strains (Kim *et al.*, 2010; Sun and Rogers, 2007; Watanabe, 2012;

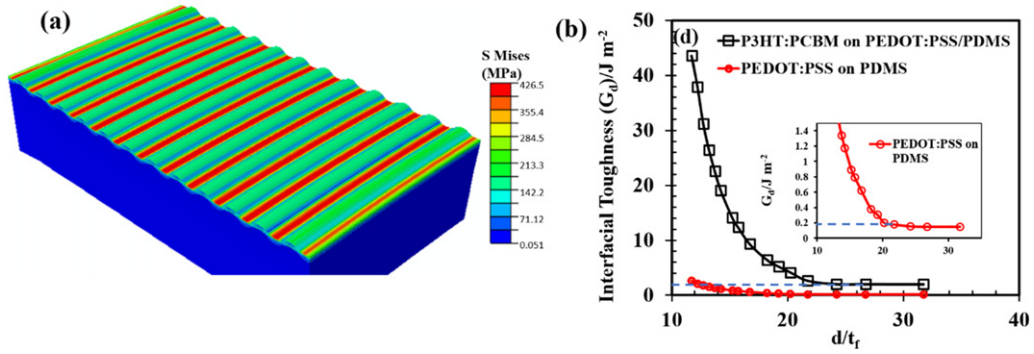

Fig. 3 (a) Von Mises of stretched stretchable P3HT:PCBM/PEDOT:PSS/PDMS, showing distribution of stresses (b) Interfacial toughness between the adjacent layers of stretchable solar cells as a function of the crack length. Interfacial toughness between PEDOT:PSS and PDMS (inset). Reproduced from Oyewole, Oluwaseun, Oyewole, Deborah, Oyelade, Omolara, *et al.*, 2020. Failure of stretchable organic solar cells under monotonic and cyclic loading. Macromolecular Materials and Engineering 305 (11), 2000369, with the permission of Wiley Publishing.

Watanabe *et al.*, 2002). The analytical solutions for the bucking geometry and maximum strain have also been obtained in buckled thin film using nonlinear buckling model. Sun *et al.* (2007) have also analyzed the incompressible substrate deformation of a folding wrinkled structures using neo-Hookean non-linear elasticity, while the nonlinear analyses of wrinkle formation in films bonded to compliant substrates have been presented by Huang *et al.* (2005).

Delamination-induced buckling and interfacial cracking in stretchable thin film

During the cyclic and monotonic deformation of stretchable electronic structure, one of the common failures is delamination (Asare *et al.*, 2017; Mei and Huang, 2013; Nolte *et al.*, 2017; Oyewole, 2015; Stafford *et al.*, 2004, 2006; Toth *et al.*, 2013; Wang *et al.*, 2017; Watanabe *et al.*, 2002; Wu *et al.*, 2013; Yoo *et al.*, 2002). The onset delamination of thin films from the polymeric substrate can induce buckling of the films and interfacial cracking that can lead to failure under deformation. For an idealized delamination of wrinkled thin films in a bi-layered structure of a wrinkled thin film on a polymeric substrate (**Fig. 2**(a)), a level of strain range during cyclic loading can initiate interfacial and film cracking (**Fig. 2**(b)). The interfacial delamination and cracking usually occur when the energy driven the failure has exceeded the critical interfacial energy release rate.

The interfacial and film cracks can continue to grow upon subsequent repeated deformation of the wrinkled or buckled stretchable thin films can lead to fatal delamination (Mei and Huang, 2013; Wang *et al.*, 2017) and other sub-critical cracking mechanisms (**Fig. 2**(c)). Assuming that the onset of film buckling corresponds to the onset of unstable interfacial crack growth, then film buckling will occur when the tractions due to buckling result in crack driving forces that exceed the adhesion/interfacial fracture energies.

The energy release rate, G_d, due to delamination of the film, can be expressed as a function of residual strains,ε, the thicknesses, t_f and t_s, of the films and substrates, and the Young's moduli,E_f andE_s, of the films and substrates, respectively. This is given by Oyewole *et al.* (2020)

$$G_d = f\left(\frac{\overline{E}_s}{\overline{E}_f}, \frac{t_s}{t_f}, \frac{d}{t_f}\right)\overline{E}_f \varepsilon^2 t_f \tag{14}$$

where $\overline{E}_s = E/\left(1-\nu_s^2\right)$, $\overline{E}_f = E/\left(1-\nu_f^2\right)$ and d is the half of the interfacial crack between the buckled film and substrate (as shown in **Fig. 2**(d)-(e)). The critical energy release rate, G_{dc}, under steady-state conditions can be considered as the interfacial toughness (Jia *et al.*, 2011; Tucker *et al.*, 2009).

Root Cause of Failure of Stretchable Electronic Devices During Operation

The failure of stretchable electronic structures depends on the design of the intrinsically non-stretchable layered films that are deposited on stretchable substrates. The root cause failure of these electronic systems varies during operation. This section explores root cause failure of different designs of stretchable electronic structures under operating conditions.

Wavy Design Structures

One way of making non-stretchable materials stretchable is through wavy design of structures. The wavy structure can be obtained on the surface of the elastomeric substrate by pre-stretching the substrate before that deposition of rigid thin film on it. When the strain is released, the stiff thin film buckles and form wrinkling structure on the substrate (Lipomi *et al.*, 2011; Oyewole *et al.*, 2015c; Oyewole, 2015; Oyewole *et al.*, 2020; Song *et al.*, 2008a). This enables the stiff thin film to be flexible and stretchable. This approach has been used extensively to achieve stretchability of non-stretchable rigid and brittle semiconductors and metals.

The applied pre-strain to the elastomeric substrate and its eventual removal after the thin-film has been deposited on it will lead to buckling of the compressed thin-film. This can lead to out-of-plane or lateral buckling or wrinkling of the device (Khang *et al.*, 2009; Wang *et al.*, 2017).

In the case of stretchable metallic films, electrons flow within the metallic films, causing heat generation that can lead to expansion which can cause residual stress due to thermal mismatch between the films and polymeric substrate. Also, since the structures are designed for them to be able to deform during service, stresses/strains can build up with the films. As a result of the residual and deformation stresses/strains, cracks can initiate at the interface between the films and the substrates. These cracks can grow and lead to delamination of the films after many cycles in the operating condition.

(Oyewole *et al.*, 2020) have studied the failure mechanisms of pre-wrinkled/buckled stretchable organic solar cells (SOSCs) under monotonic and cyclic loading. The failure of the optoelectronic properties of the SOSCs were attributed to the flattening of the wavy structure and the initiation/propagation of interfacial cracks which eventually lead to failure through delamination. The interfacial cracks can limit the intensity of light that is necessary for the optimum generation of holes and electrons in the SOSCs.

To further understand the failure mechanisms, the stress distributions in 3D structure have been studied (Oyewole *et al.*, 2015a) using ABACUS Software (upon releasing of the pre-strain substrate). The results show that the stresses are concentrated along the troughs and crests of the wavy structure (**Fig. 3**(a)), which are consistent with the transverse and interfacial cracks that are obtained from the experiments. Delamination-induced buckling was also observed during the deformation and ABACUS software was used to calculate the critical interfacial toughness between the adjacent layers of the stretchable structure. The critical interfacial toughness values (**Fig. 3**(b)) were obtained when the energy released rate attained the stretchable condition. The interfacial toughness between PEDOT:PSS and PDMS substrate is reported to be $\approx 0.2\ \mathrm{Jm}^{-2}$ and that between P3HT:PCBM and PEDOT:PSS is found to be $\approx 1.98\ \mathrm{Jm}^{-2}$.

Island-Interconnect Design and Mesh Structures

An alternative strategy for the development of stretchable electronics is the use of island-interconnects and/or mesh structures to induce stretchability of the electronic materials. Here, the rigid and brittle functional materials (otherwise referred to as island) are interconnected using meta interconnects or some flexible materials (otherwise referred to as bridge) to achieve stretchability of the materials on certain axes (Ko *et al.*, 2008; Lee *et al.*, 2011b; Lim *et al.*, 2014; Suarez *et al.*, 2017; Zhang *et al.*, 2013). These stretchable interconnects can be obtained through the highly malleable and compliant electronic materials, such as low-temperature liquid metal. Beside this, the interconnects can be designed in a way that mitigates the local strains from out-of-plane deformations. These can be in terms of buckled designs, pup-up interconnection designs, or serpentine-shaped designs (Kim *et al.*, 2008; Lim *et al.*, 2014; Miao *et al.*, 2011; Zhang *et al.*, 2013). The major setback with the out-of-plane structures is the challenge faced while executing them on a rapid manufacturing process, like roll-to-roll or printing methods (Wu, 2019).

So, preferably, the stretchable interconnects can be fabricated using in-plane geometries for the conductors, such as horseshoe geometries, pulse, or stretchable line (Wu, 2019). Furthermore, an improved level of stretchability can also be achieved through the use of spiral-based interconnects, instead of the serpentine-based. The entanglement within spiral has been reported to have ability to eliminate the elevation above the substrate, which is an indication that it is stretchable than its serpentine-based counterparts. Under elastic deformation, they can stretch up to 250% and they also stretch to 325% without significant failure. The serpentine-based interconnects have been widely used for various stretchable electronic systems, such as stretchable battery, skin-like temperature sensor, etc (Akre *et al.*, 2011; Kim *et al.*, 2008; Webb *et al.*, 2013; Xu *et al.*, 2013). In the serpentine structure, the stretchability can be enhanced when the structure is allowed to deform and buckle in the out-of-plane directions (Wu, 2019).

A good mesh structure with optimum stretchability (usually $>100\%$) can also be achieved by using interconnect island mechanism (Akre *et al.*, 2011; Wu, 2019; Kim *et al.*, 2008) have used this configuration to fabricate integrated circuits that can withstand extreme mechanical deformation. Their design concepts for stretchable electronics utilized ultrathin semiconductor nanomaterials (e.g., silicon ribbons) that are integrated on elastomeric substrates in noncoplanar mesh configurations. The noncoplanar structure, together with the deformable serpentine bridge design can achieve high stretchability level up to 140% strain without failure (Liu *et al.*, 2017). This design is capable of accommodating difficult configuration such as corkscrew twists with tight pitch. However, there can be failure due to cracking at the joint of interconnect and stress-induced delamination of the films from the polymeric substrate.

Fractal Design Structures

One of the major challenges in the realization of stretchable electronics for certain applications is the difficulty in achieving large stretchability and at the same time ensure large area coverage of the active devices (Ma and Zhang, 2016). Fractal-inspired geometric designs (Su *et al.*, 2015) are strategies that have been reported to mitigate this difficulty. The fractal designs of the electrical interconnects can be used to achieve greater stretchability and large area coverage of the active devices for stretchable electronics.

The simple transformation that is introduced by the fractal design could lead to changes in the macroscopic shapes of the materials and this results in higher stretching performance. This provides new opportunities for integrating high performance electronic materials. Cho *et al.* (2014) have introduced patterns that enable the exact control of the differentiated material

structure. The work presented modification of materials through hierarchical cut patterns that accommodate for extremely large strains with shape changes that involve a large range of macroscopic shapes. The electrode produced from this approach can stretch to over 800% of the original area with the application of little strain. The approach has widened the design space for materials' tunability which have applications devices that require flexibility and stretchability such as stretchable energy devices, bio scaffolds, and photonics.

Generally, fractal designs geometries have applications in high performance electronic materials that are used with energy (i.e., lithium-ion batteries, Solar Cells, LED), biomedical areas (i.e., epidermal electronics: human skin, organs, and various tissues etc). (Fan *et al.*, 2014; Ma and Zhang, 2016).

Origami and Kirigami Structures

Foldable electronics is one of the key technologies for the next generation of portable displays and wearable electronics (Kim *et al.*, 2016). Since high strain is involved during folding and unfolding of the foldable devices, the substrates and the conductive interconnects used in such devices must possess outstanding stretchability, coupled with low resistance during operation (Kim *et al.*, 2016; Nogi *et al.*, 2013). This led to the concept of Origami design. Origami is an art of folding paper to achieve specifically designed grooves. Hence, origami structural electronics are suitable for achieving high stretchability involved in foldable electronics.

The origami electronics can be fabricated by fabricating the devices directly on foldable substrates or by transfer of prefabricated devices on existing rigid substrates onto other foldable substrates. Although, the former is desirable as it has relatively low yield of transfer process, plastics have low melting point and high thermal expansion coefficients. These can limit the processing temperature, unlike what is obtainable in other rigid substrates (i.e., silicon, glass) (Kim *et al.*, 2016).

Kim *et al.* (2016) have also adopted transfer-free fabrication processes, which were carried out at high temperatures to fabricate foldable integrated array of thin film transistors (TFTs)for next-generation displays. The origami structures have been used widely in manufacturing foldable conductors, stretchable lithium batteries (LIBs), supercapacitors and paper antennas (Kim *et al.*, 2016; Nogi *et al.*, 2013).

Kirigami is a variation of origami which combines folding to cutting. It is a Japanese technique of paper cutting where strategic cutting will change the morphology of a structure (Shyu *et al.*, 2015; Wu, 2019). This approach can be used to enhance stretchability of electronic materials (e.g., graphene) as it transforms the elastic behavior of inextensible substrate to highly tensile one. This is achieved by making parallel cuts and divide them into an array of thin strips with short connections. The kirigami structures have been applied to bulk materials as well as nanomaterials. The influence of kirigami structures on the stretchability of graphene has been widely reported. It has also been used to enhance the stretchability of molybdenum disulfide (MoS_2). The results show that kirigami structure can be used to improve the yield and fracture strains of monolayer MoS_2, even beyond the success recorded in monolayer graphene (Guo *et al.*, 2014; Hanakata *et al.*, 2016; Qi *et al.*, 2014).

For instance, this structure has been used to fabricate LIBs whose stretchability is enhanced up to 150% of its original state (Song *et al.*, 2015). Also, a network of kirigami structural notches have been applied to rigid nanocomposites and other inextensible sheets. This improves the ultimate strain of the final sheets significantly from 4% to 370%, and protected them from uncertain local failures (Shyu *et al.*, 2015).

It should be noted that to achieve most of the strategies discussed above, the fabrication processes require temperature treatment and application of stresses/strains during manufacturing and/or operation. Hence, one of the key factors that lead to failure of the devices is the mismatch between the mechanical behavior of layers which are in contacts. These mechanical behaviors are the coefficient of thermal expansion, α, the Young's modulus, E, Poisson's ratio, v, and toughness.

The coefficient of thermal expansion, α, describes the thermal expansion properties of a material. It describes the geometry change in the material in response to changes in temperature. This becomes very important when the fabricating procedure require high temperature (i.e., during annealing, deposition, or transfer of film to substrates or other layers). The α mismatch between the films or between layers can lead to generation of interfacial stress especially while cooling to ambient condition. This interfacial stress produces cylindrical rolling in flexible and stretchable electronics. This temperature-induced curvature and α mismatch between the substrate and the film can lead to overlay error within the interlayers and between substrate and adjacent film. This can cause debonding and delamination of the films which will cause failure of the entire device.

Design of Flexible/Stretchable Electronic Structures

Overview

This section presents the designs of flexible/stretchable inorganic, organic and hybrid organic-inorganic electronic structures. These include flexible/stretchable metallic thin films; stretchable organic solar cells, and stretchable organo-metallic perovskite light emitting devices. Most of the layers of these electronic structures undergo failure under deformation (stretching, bending and twisting) because they are intrinsically not deformable (Asare *et al.*, 2015; Kaltenbrunner *et al.*, 2012; Lipomi *et al.*, 2011, 2012; Oyewole, 2015; Oyewole *et al.*, 2020; Sekitani *et al.*, 2008, 2009). Some of these layers exhibit low strain-to-failure under deformation. Hence, flexible/stretchable of these electronic structures are designed by dispersing the intrinsically non-flexible/

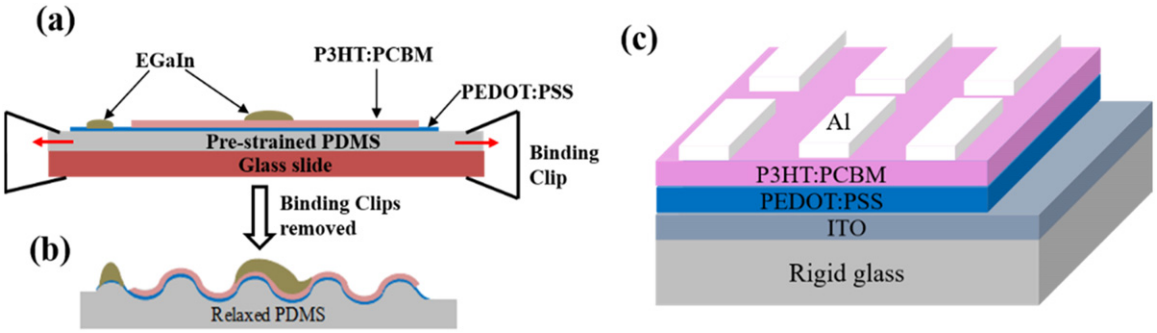

Fig. 4 Typical simple architecture of (a-b) stretchable organic solar cells and (c) rigid organic solar cells. Reproduced from Oyewole, Oluwaseun, Oyewole, Deborah, Oyelade, Omolara, *et al.*, 2020. Failure of stretchable organic solar cells under monotonic and cyclic loading. Macromolecular Materials and Engineering 305 (11), 2000369, with the permission of Wiley Publishing.

stretchable structures in polymeric materials that enhance deformability. The layers can also be deposited on pre-stretched polymeric materials to form wrinkled/buckled structures, which can deform out of plane without inducing strains in layered structures.

Design of Flexible/Stretchable Organic Solar Cells

A typical architecture of stretchable organic solar cells (**Fig. 4**(a)-(b)) consists of polymeric photoactive layer that is deposited on poly(3,4-ethylenedioxythiophene):polystyrene sulfonate (PEDOT:PSS). The photoactive layer is made of bulk heterojunction structures which is a blend of poly(3-hexylthiophene):phenyl-C61-butyric acid methyl ester (P3HT:PCBM) (Agyei-Tuffour *et al.*, 2017b; Asare *et al.*, 2015; Lipomi *et al.*, 2011, 2012; Oyewole, 2015; Oyewole *et al.*, 2020; Yu *et al.*, 2014b). The PEDOT:PSS serves as the anodic layer in this configuration. In a regular rigid structure of the organic solar cells, Indium Tin Oxide (ITO) is usually used as the anodic conducting oxide (Yu *et al.*, 2014b). **Fig. 4**(c) presents a typical rigid structure of organic solar cells. It is important to note that the strain to failure of ITO is very low, making it difficult to be adopted in stretchable solar cells. However, ITO has a very good interfacial adhesion on PET, making widely used for flexible electronic structures (Asare *et al.*, 2015; Baran *et al.*, 2020; Cao *et al.*, 2012; Liu *et al.*, 2014, 2017; Logothetidis, 2008; Someya and Sekitani, 2009; Yu *et al.*, 2014b) The interfacial integrity and the optoelectronic properties of the flexible films depend on the bending radius during deformation.

One route to design a robust stretchable organic solar cell is by fabricating the structures in a way that the net strain in the layered films is reduce during cyclic and monotonic deformations. **Fig. 4**(a) presents a typical design of stretchable organic solar cells. The constituent layers of the device are deposited on pre-stretched polymeric materials such that it forms wavy-like structure when the strain is removed (**Fig. 4**(b)). The common polymeric materials that is widely used for stretchable organic solar cells is Poly-di-methyl-siloxane (PDMS). This can be fabricated by mixing a Sylgard 184 silicone elastomer base with a Sylgard 184 silicone elastomer curing agent in a 10:1 wt ratio. The mixture is usually degassed in a vacuum oven of pressure of about 25 kPa for 60 min to remove the trapped bubbles (Lipomi *et al.*, 2011, 2012; Oyewole *et al.*, 2015a; Oyewole *et al.*, 2020). For smooth surface of the PDMS, a curing mode made with a shining silicon wafer base have been used to cure PDMS at 65 °C for 2 h (Lipomi *et al.*, 2011, 2012; Oyewole *et al.*, 2015a, 2020). A thickness of 0.5 mm of the mold has been used by Oyewole *et al.* (2020) to enhance flexibility.

For the deposition of layers of stretchable organic solar cells, the PDMS ($20mm \times 30mm \times 0.5mm$) can be slowly pre-stretched and attached to a glass slide (Oyewole *et al.*, 2020). It is important to orient the cured PDMS surface (against the silicon wafer) with its face exposed to the atmosphere before cleaning with a UV/Ozone cleaner or Ozone plasma. The layered PEDOT:PSS and P3HT:PCBM can then be deposited using spin coating method before dropping a E-GaIn. The wrinkled stretchable organic solar cells are then formed by releasing the pre-stretched strain from PDMS substrate.

Precursor preparation and deposition of PEDOT:PSS and P3HT:PCBM on PDMS

To prepare and deposit PEDOT:PSS on pre-stretched PDMS substrate, a mixture of PEDOT:PSS (PEDOT:PSS, H. C. Starck, Newton, MA, USA), dimethylsulfoxide (DMSO, MiliporeSigma, MO, USA) and Triton X-100 (Triton, MiliporeSigma, MO, USA) was prepared with a volume ratio of 94: 5: 1. The dimethylsulfoxide was added to segregate the weak PSS for strong inter-PEDOT bridging. This increased the conductivity of PEDOS:PSS on PDMS. Triton X-100 was also added to increase the wettability of the PEDOT:PSS on PDMS. The mixture was then filtered using a 0.45 μm mesh filter before spin-coating onto the pre-stretched PDMS at 1000 revolutions per minute (rpm) for 50 s. It resulted in a uniform transparent film with a thickness of ~100 nm. The spin-coated PEDOT:PSS film was then annealed in air at 100 °C for 10 min. It was then transferred into a nitrogen filled glove box.

The active P3HT:PCBM layer was prepared and spin coated in the glove box. A 30 mg mL^{-1} P3HT:PCBM (1:1 wt%) solution was spin coated onto the PEDOT:PSS at 800 rpm for 30 s and 3000 rpm for 50 s to achieve a thin film of ~120 nm thick. The solution was prepared by mixing P3HT (P3HT, Sigma Aldrich, regioregular, average M_w 20,000–45,000) and PCBM (PCBM, Sigma

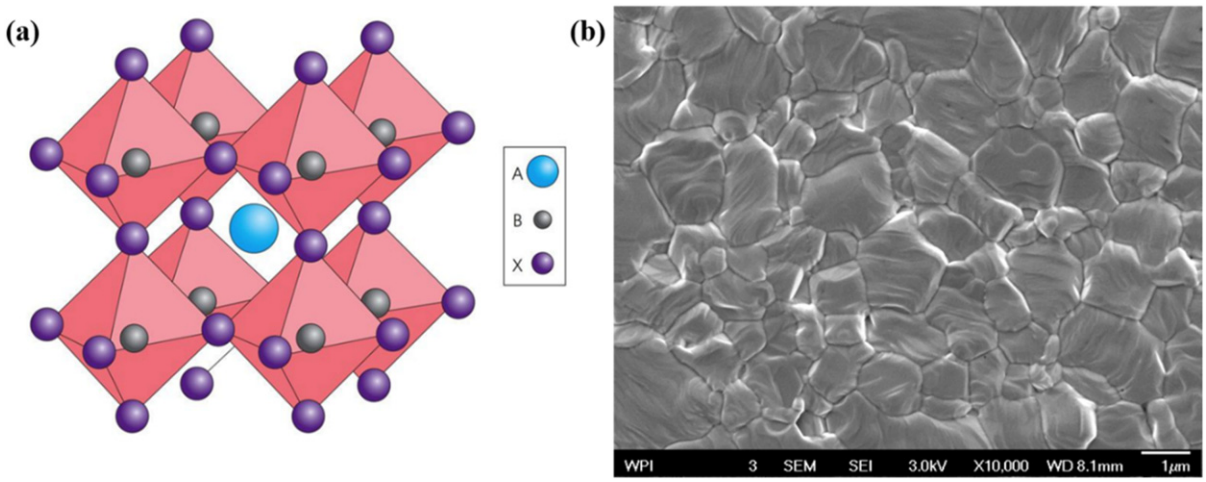

Fig. 5 Structure of perovskite: (a) ABX_3 structure and (b) SEM image of perovskite film showing interlocking grains. Reprinted from Green, Martin A., Anita, Ho-Baillie, and Snaith, Henry J., 2014. The emergence of perovskite solar cells. Nature Photonics 8 (7), 506–514, with permission of Macmillan Publishers Limited.

Aldrich, > 99.5%) in anhydrous chlorobenzene. The spin-coated P3HT:PCBM layer was annealed at 120 °C for 10 min. A cross-sectional scanning electron microscopy (SEM) can be used to determine the thickness of the spin coated film.

Design of Flexible/Stretchable Perovskite Light Emitting Devices

Perovskite light emitting devices consist of a perovskite compound having a general chemical formulas ABX_3 (**Fig. 5**(a)), where A is an organic cation residing at the 8 corners of the cubic cell, and B is a metal cation located at the body center of the cell, and X is a halide anion (Green *et al.*, 2014). Usually, the A cation could be Cs^{2+}, Ca^{2+}, positively charged organic compounds like methylammonium, $CH_3NH_3{}^+$ (MA^+) or formamidinium, $CH(NH_2)_2{}^+$ (FA^+). The metal cations which are usually smaller in size than the organic cation could be Pb^{2+}, Ti^{4+}, Sn^{2+}, and the anion is usually I or Br.

The perovskite thin films are interconnection of grains (**Fig. 5**(b)) which can easily fail under deformation. It is also important to note that formation of pre-wrinkled structure of perovskite like stretchable organic solar cells could be very difficult due the locking of grains which may fail under monotonic and cyclic deformations. To design a robust stretchable perovskite light emitting device, both the intrinsically non-stretchable perovskite and PEDOT:PSS films can have been modified with poly(ethylene oxide) (PEO).

Fabrication procedure for perovskite light emitting devices

Fabrication of perovskite light emitting devices requires a PDMS substrates, PEDOT:PSS and perovskite precursors and E-GaIn. The fabrication of PDMS substrates is similar to the techniques described by Oyewole *et al.* (2020). After cleaning the surface of the PDMS using an oxygen plasma, a composite from the mixture of aqueous PEDOT:PSS and PEO solution can be spin coated. The composite PEDOT:PSS serves as the anodic layer of the PeLEDs which can be prepared by mixing PEDOT:PSS, DMSO, and Triton X-100 in volume ratio of 93:5:2, respectively. Addition of DMSO solution improves the conductivity of PEDOT:PSS while TritonX-100 improves its wettability on PDMS. (Oyewole *et al.*, 2020) To make the PeLEDs fully stretchable, the anodic PEDOT:PSS layer is usually doped with PEO. The PEO can be prepared in form of a solution by dissolving PEO powder in DMF to give a concentration of 10 mg mL^{-1}. Then, the PEDOT:PSS–PEO composite was obtained by using 33 wt% PEO as optimized by Bade *et al.* (2017) The mixture was stirred for 2 h at 1500 rpm to ensure homogeneous mixture (as shown in **Fig. 6**(a)). This produced stretchable PEDOT:PSS solution that was spin-coated on the treated PDMS substrates at 2000 rpm for 30 s. The resulting films were annealed at 110 °C for 10 min on a hot plate.

For a typical PeLEDs, the emitting layer can be made from a mixture of lead bromide and methylammonium bromide with the incorporation of PEO to enhance stretchability. The precursor solution for emitting layer is prepared by dissolving $PbBr_2$ and CH_3NH_3Br (in molar ratio of 1:1.5, respectively) in anhydrous DMSO to obtain $MAPbBr_3$ solution with concentration of 500 mg mL^{-1} The solution was stirred for 30 min at 70 °C and it was filtered using a 0.45 μm mesh. The PEO solution was then mixed with the filtered $MAPbBr_3$ solution in the ratio of 1:39 (wt%), (Kim *et al.*, 2020) respectively, to form $MAPbBr_3$–PEO composite emitter that can be stretched. The mixture was also stirred at 70 °C for 30 min and was spin-coated on the PEDOT:PSS–PEO/PDMS substrates at 1500 rpm for 60 s (as shown in **Fig. 6**(b)). This was followed by thermal annealing at 80 °C for 5 min. Finally, a drop of Eutectic Gallium Indium (E-GaIn) was dispensed on the perovskite film through a syringe (**Fig. 6**(c)) before removing the stretchable layered structure (**Fig. 6**(d)) from the support glass slide.

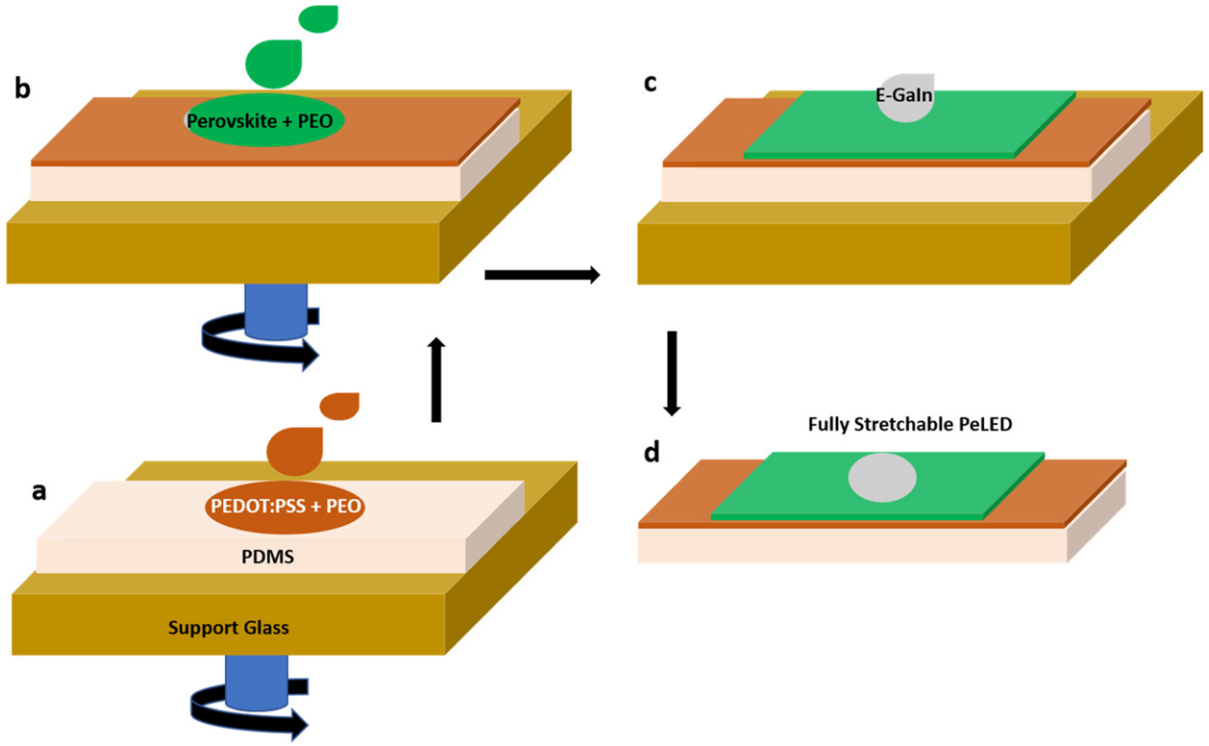

Fig. 6 Schematics of fabrication process of fully stretchable PeLEDs, showing the deposition of (a) PEDOT:PSS-PEO composite, (b) perovskite-PEO composite, (c) cathodic eutectic Indium gallium) and (d) the final fully stretchable PeLEDs.

Fatigue Test and Analysis in Stretchable Electronic Structures

Fatigue test in FSE structures is performed in the regime of low cycle fatigue (LCF) in such a way that the thin films are plastically strain in each cycle. Hence, plastic strain range ($\Delta\varepsilon$) can be related to the lifetime (N_f) of the films using Coffin-Manson relationship Eq. (15) (Kraft *et al.*, 2001; Suresh, 1999)

$$\frac{\Delta\varepsilon}{2} = \varepsilon_f^{'}(2N_f)^c \tag{15}$$

Where $\varepsilon_f^{'}$ and c are the fatigue ductility coefficient and exponent, respectively. Materials with higher ductility exponent can accommodate higher repeated strains before failure.

A MicroTester is the suitable equipment for fatigue testing in FSE structure using Instron in-built Test Profiler. For Eq. (1) to be used in the analysis, a load control fatigue test is essential for estimation of plastic strain range to failure in the materials. It is important to note that FSE structures are layered thin films on stretchable substrate. Therefore, a comparison of strain range versus fatigue lifetime is necessary between the stretchable substrates and the layered FSE on the stretchable substrate.

In the case of stretchable organic solar cells (SOSCs), Oyewole *et al.* (2020) have carried out fatigue test under load control, comparing a PDMS substrate and the layered SOSCs. The strain ranges can be obtained by subtracting the minimum strain from the maximum strain in **Fig. 7**(a). The plastic strain ranges versus fatigue lifetime curves are presented in **Fig. 7**(b), for the different loads for SOSC structures. As shown in **Fig. 7**(b), the strain range of the PDMS substrate is ~30% for over 4000 cycles at maximum load of 7 N while the strain ranges of the coated-PDMS structures were smaller initially over a certain number of cycles before increasing. This is because the coated PDMS substrates are stiffer than the bare PDMS substrates. The lifetimes (N_f) of the layered SOSC structures can be characterized as number of cycles at the onset of the increasing strain range.

The strain ranges and lifetimes of the SOSC structures can be incorporated into Eq. (1) to obtained fatigue ductility exponent, c, which is a key parameter to describe the extend at which the SOSC structure can accommodate repeated strains before failure. A typical log-log of strain range-lifetime curve of SOSCs is shown in **Fig. 7**(c). The fatigue ductility exponent is basically the slope of the curve. The value of c has been estimated to be − 0.3 for pre-wrinkled SOSC structures (Oyewole *et al.*, 2020), between − 0.4 for stretchable metallic thin film of Cu (Kraft *et al.*, 2001) and − 0.04 for fully stretchable perovskite light emitting devices.

Typical Fatigue Testing for SOSCs

The fatigue test on SOSCs is performed using MicroTester that is instrumented with a small load cell for better sensitivity. Fatigue tests have been carried out using a MicroTester that was instrumented with a 50 N load cell (Oyewole *et al.*, 2020).

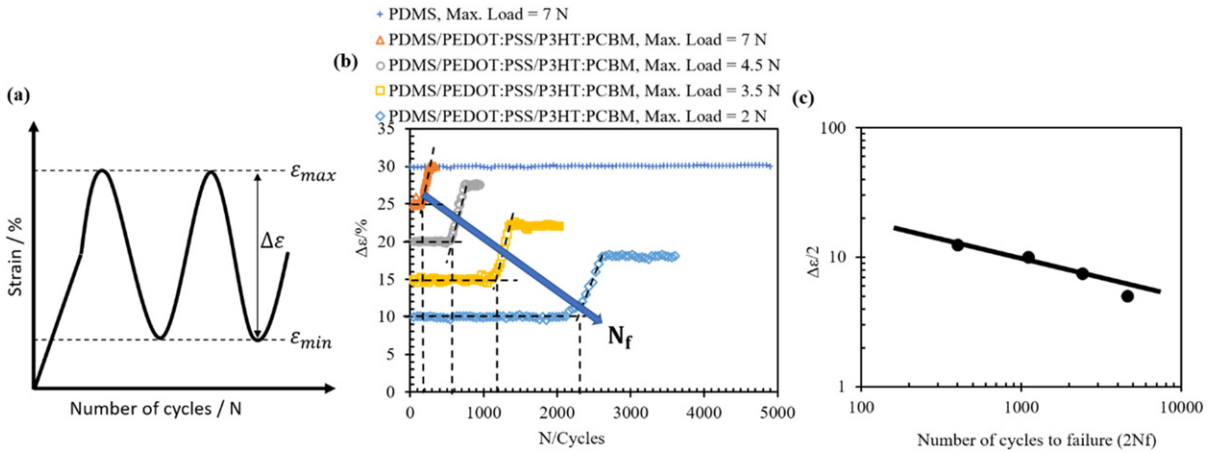

Fig. 7 Fatigue behavior of layered stretchable organic solar cells: (a) Schematic of a typical strain-number of cycle that shows the both the minimum and maximum strains, (b) Strain range - number of cycles ($\varepsilon - N$) at different loads; downward arrow indicates the increase in the number of cycles to failure as the strain range decreases and (c) Log-Log plot of strain amplitude - number of cycles to failure [b and c are. Reproduced from Oyewole, Oluwaseun, Oyewole, Deborah, Oyelade, Omolara, *et al.*, 2020. Failure of stretchable organic solar cells under monotonic and cyclic loading. Macromolecular Materials and Engineering 305 (11), 2000369, with the permission of Wiley Publishing.

First, the polymeric PDMS substrates were cyclically deformed under a loaded control between 0 N and 7 N to obtain a strain range of ~30% in uniaxial direction. The fatigue tests were then performed on layered SOSCs between minimum load of 0 N and maximum loads of 2–7 N. Based on these loading conditions, the SOSC structures were then strained with total strain ranges between 10% and 25%. These strain ranges were estimated and plotted versus the number of cycles for further analysis.

Fatigue Failure in Flexible/Stretchable Electronic Devices

Failure in Flexible/Stretchable Metallic Films

Metallic films are usually deposited on polymeric substrate using thermal evaporation, electron beam and sputtering techniques which require high temperature. In a scenario whereby, the substrate is a PDMS that was pre-stretched before deposition, stress-induced failure is foreseen after release of strains. Wavy-like wrinkled profiles are induced after the release of the strain from the pre-strained PDMS. A typical wrinkled gold film on PDMS substrate is presented in **Fig. 1**(a)-(c). The images show that the wavelengths of the wrinkled structure are dependent on the pre-strain values (Oyewole *et al.*, 2015a). The wavelengths reduced from 9.7 μm, for a pre-strain of 18%, to 6.6 μm, for a pre-strain of 36%, and 3.0 μm, for a pre-strain of 70%. Hence, the wavelengths are inversely related to the pre-strain values (**Fig. 8**). At the pre-strain of 70%, transverse cracks are very evident (**Fig. 1**(c)).

The type of materials used for the substrate would determine the nature of wrinkling and stress concentration in stretchable metallic films, which can affect fatigue failure. The increase in the elastic modulus of the substrate increases the concentration of stress in the wrinkled structure (**Fig. 9**(a)-(d)). The wrinkling profile is well defined with increasing substrate Young's modulus (Oyewole *et al.*, 2015a). However, there is a high possibility that failure would be induced by the higher Von Mises stresses in the wrinkled Au-PDMS structures that have higher moduli. Hence, a balanced approach is needed to obtain well defined wrinkled profiles without inducing failure.

Fatigue failures in stretchable metallic films are also driven by prior delamination-induced buckling (which is common to most metallic island thin films). The delamination-induced are induced by residual stresses in the Au films due to the thermal expansion coefficient mismatch between thermally evaporated metal and the stretchable polymeric substrate (Oyewole *et al.*, 2015a). Hence, the critical stresses for different wavelengths are important. In the case of Au-PDMS structure, the critical stresses for the onset of wrinkling/buckling have been estimated (Oyewole *et al.*, 2015a). The critical stress decreases with increasing wavelength and vice-versa (**Fig. 10**(a)). Therefore, the critical stress is inversely related to the wavelength of the buckling/wrinkling profile (Oyewole *et al.*, 2015a).

In the case of stretchable thin films of Cu and Ag on polyimide substrates, fatigue failures are dominated by formation of extrusion within large grains while intergranular cracks have been found within the fine grain regions (**Fig. 10**(b)-(c)) (Kraft *et al.*, 2001). It has also been found that there are formation of large voids underneath the extrusions along the interface between the thin films and the substrates (Kraft *et al.*, 2001).

Failure in Stretchable Organic Solar Cells and Light Emitting Devices

Due to the nature of organic materials, stretchable organic solar cells are formed by pre-stretching the substrate (as presented in Section "Mechanics of 2D Wrinkling"). The underlying failure mechanisms in the cyclically deformed solar cell structures include

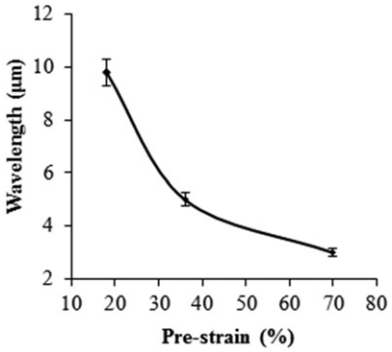

Fig. 8 The wavelength of wrinkle profile versus pre-strain value of the PDMS substrate. Reproduced from Oyewole, O.K., Yu, D., Du, J., *et al.*, 2015a. Micro-wrinkling and delamination-induced buckling of stretchable electronic structures. Journal of Applied Physics 117(23), with permission of AIP Publishing.

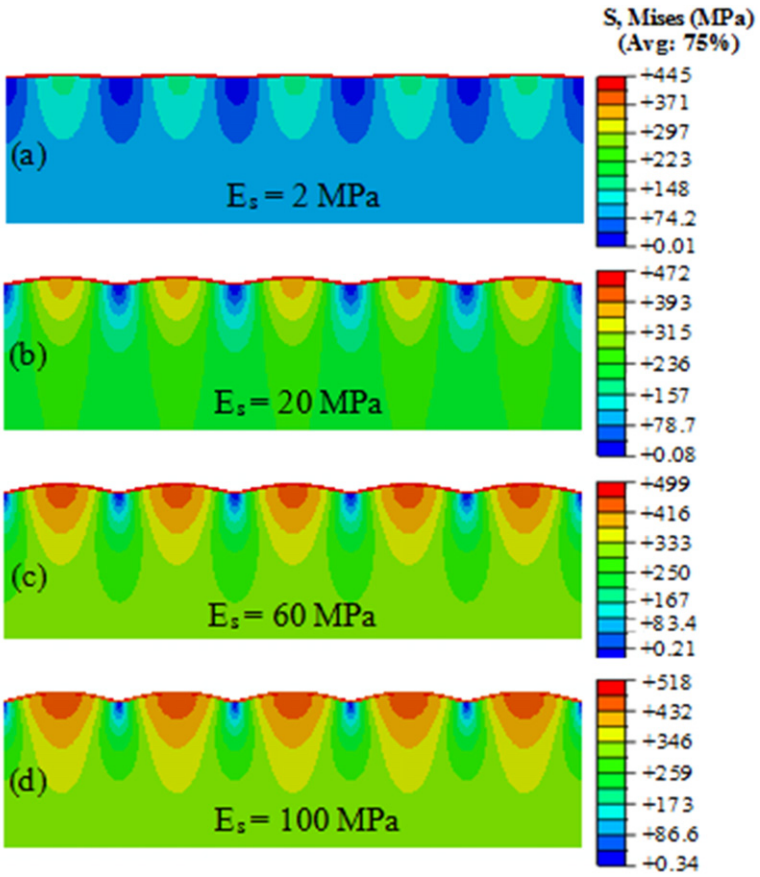

Fig. 9 Von Mises showing the dependence of elastic modulus of the substrate on wrinkle profile of Au film on PDMS substrate at 36% pre-strain. Reproduced from Oyewole, O.K., Yu, D., Du, J., *et al.*, 2015a. Micro-wrinkling and delamination-induced buckling of stretchable electronic structures. Journal of Applied Physics 117 (23), with permission of AIP Publishing.

delamination-induced buckling (Oyewole *et al.*, 2020), wrinkling, film debonding and cracking. The level of failure depends on the strain ranges in the strain-life relation for the layered structures. Typical scanning electron microscopy (SEM) images (**Fig. 11**) compare the as-prepared layered structures of stretchable organic solar cells (**Fig. 11**(a)) to those that were cyclically deformed to different strain levels (**Fig. 11**(b)-(d)). Cracks are quite evident in the layered structures when the stretchable films were subjected to 1900 cycles of cyclic deformation at strain range of 10% (**Fig. 11**(b)). At higher strains between 10% and 25%, the cracks initiate from the higher concentration of stresses within the troughs and crest of the corrugations (**Fig. 11**(c)) which can lead to delamination and debonding (**Fig. 11**(d)) (Oyewole *et al.*, 2020). Cracks have also been seen in the anodic layer of stretchable organic

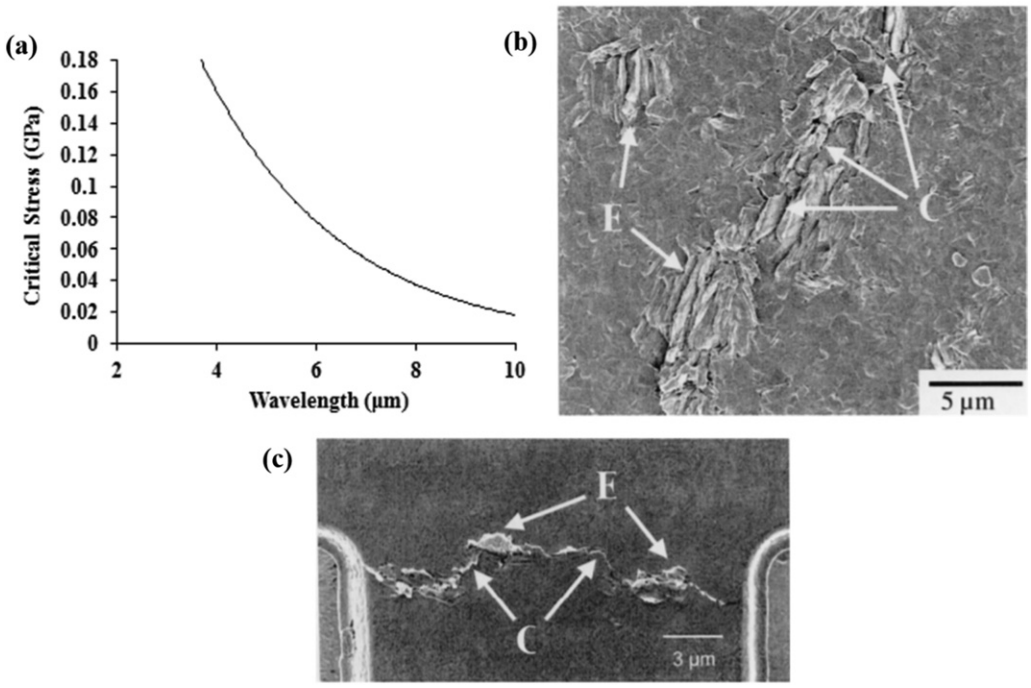

Fig. 10 (a) Dependence of profile wavelength on critical stress, (b-c) Fatigue failure of Cu and Ag thin films; (a) Focused ion beam micrograph of a 3 m thick Cu film on a polyimide substrate, large extrusions and cracks are marked by E and C, respectively. (b) SEM micrograph showing of Ag thin film, large extrusions (marked by E) are connected by a crack (C) [b and c are reprinted from Kraft. Reproduced from (a) Oyewole, O.K., Yu, D., Du, J., *et al.*, 2015a. Micro-wrinkling and delamination-induced buckling of stretchable electronic structures. Journal of Applied Physics 117 (23), with permission of AIP Publishing. (b and c) Kraft, O., R. Schwaiger, and P. Wellner. 2001. Fatigue in thin films: Lifetime and damage formation. Materials Science and Engineering A 319–321, 919–923.

solar cells at 20% strain (Oyewole *et al.*, 2020). However, the underlying stretchable substrates seem not to experience fatigue damage after over 4000 cycles at 30% strain range (Oyewole *et al.*, 2020).

In the case of stretchable light emitting devices, the perovskite crystals are embedded within the PEO matrix (**Fig. 12**) to allow stretching. In a typical stretchable PeLED cell that was cyclically deformed up to1000 cycles, cracking failure is more dominant compared to other failure mechanisms within the PEO matrix. Compared to the as-prepared layered structure (**Fig. 12**(a)), cracks increase with increasing strain (**Fig. 12**(b)-(d)) in the cyclically deformed structures. The cracks are deflected by undissolved PEO and the isolated perovskite crystals.

Effects of Fatigue Failure on Stretchable Electronic Structures

Electronic devices experience fatigue during service conditions. One way of understanding the reliability of stretchable electronic structures, during cycles of deformation, is by exploring the effects of the fatigue failure on their optoelectronic properties. The effects of the observed fatigue failure on various optoelectronic properties of stretchable electronic structures are presented in this section.

Effects of Fatigue Failure on Optical Properties

Failures due to cyclic deformation have significant effects on the optical properties of FSE structures. In the case of stretchable solar cells, performance is dependent on the amount of light that the photoactive material can trap. Essentially, the light travels through the transparent anodic PEDOT:PSS layer. The optical transmittance of electronic structures can be measured using a UV–vis–NIR spectrophotometer (Avantes BV, USA). In pre-wrinkled stretchable PEDOT:PSS, optical transmittance initially increases with increasing strain ranges, before a decrease in the transmittance at higher applied strains (**Fig. 13**(a)). The initial increase in the transmittance is attributed to the flattening of the wrinkled films at moderately strains (**Fig. 13**(b)-(c)). However, when the films are over-stretched, the transmittance decreases due to formation transverse cracks (**Fig. 13**(d)). The surface and interfacial microcracks are capable of scattering light, which can then reduce the intensity of light that is meant for the generation of holes and electrons in the cells.

In the case of fully stretchable PeLED structures, the transmittance of PEO doped PEDOT:PSS reduced with increasing strain range (**Fig. 14**(a)) due to the observed transverse cracks within the PEO matrix. However, the transmittance bounces back when the

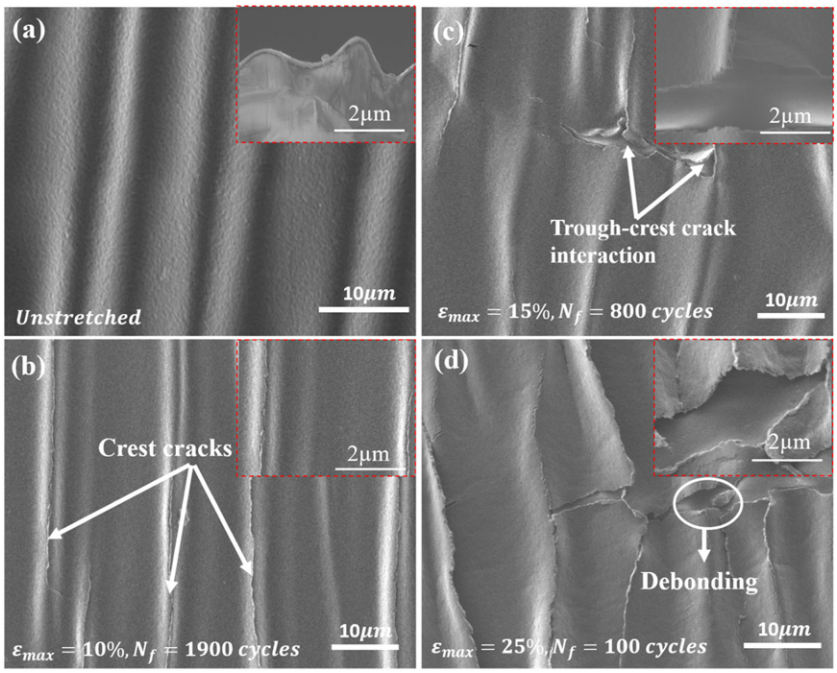

Fig. 11 SEM images of fatigue failure modes of layered stretchable organic solar cell structure: (a) top surface of as-prepared films with the cross-section of the layered structure (inset), (b) after 1900 cycles to failure with maximum strain of 10% with evidence of fatigue cracks along the crest of the wavy structure; (c) after 800 cycle to failure at 15% strain with evidence of crest-trough inter-cracking due to fatigue, and (d) after 100 cycles at 25%, showing delamination and debonding of films (inset). Reproduced from Oyewole, Oluwaseun, Oyewole, Deborah, Oyelade, Omolara, *et al.*, 2020. Failure of stretchable organic solar cells under monotonic and cyclic loading. Macromolecular Materials and Engineering 305 (11), 2000369, with the permission of Wiley Publishing.

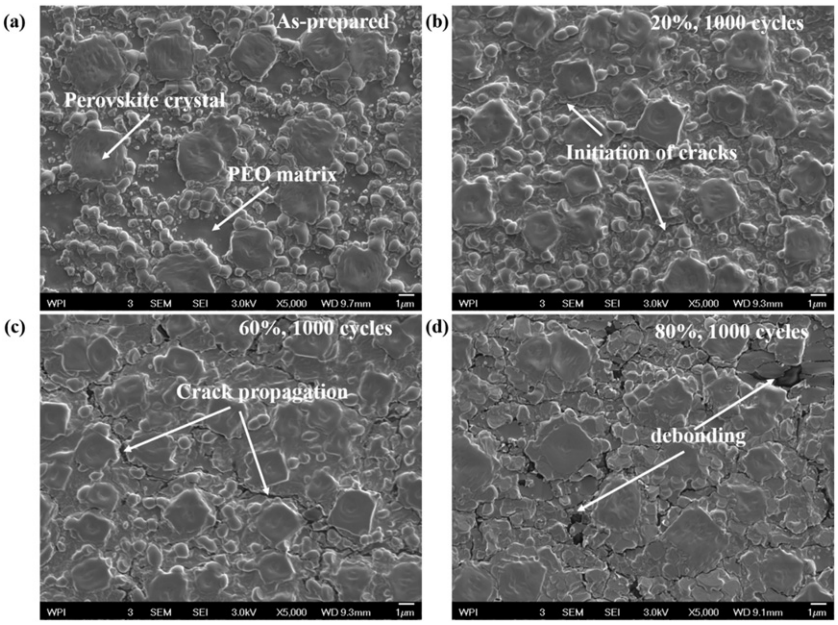

Fig. 12 SEM images of fatigue failure in layered perovskite light emitting device structures: (a) As-prepared structure, perovskite crystals are clearly embedded within PEO matrix, (b-d) Cyclically deformed structures at: (a) 20% strain that shows initiation of cracks within the PEO matrix, (c) 60% strain with clear propagation of cracks within the PEO matrix, (d) 80% strain that show catastrophic fatigue damage, films start to debond from the substrate.

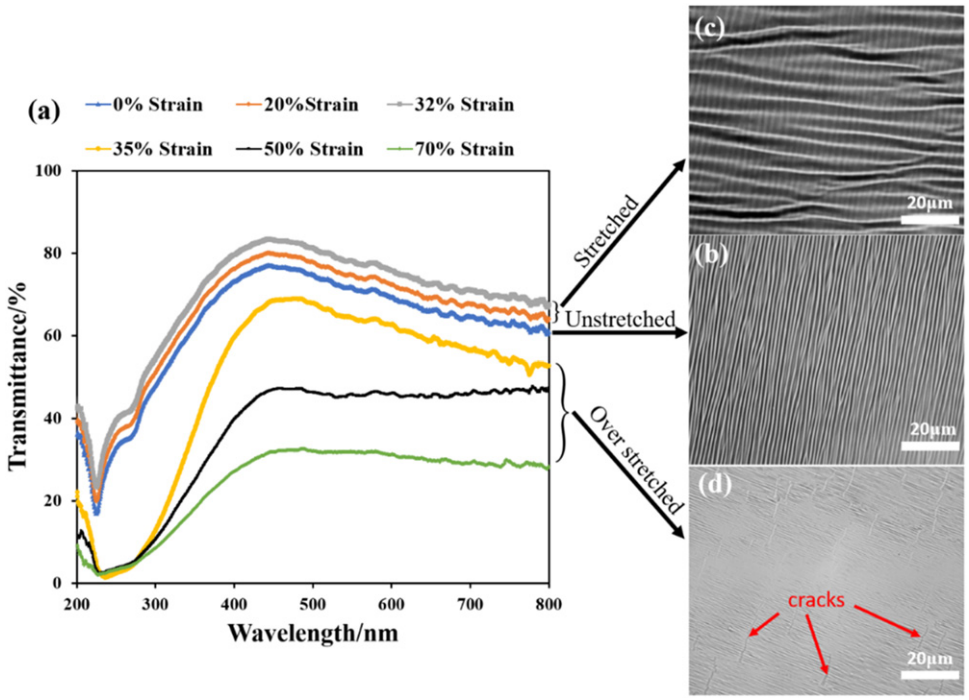

Fig. 13 (a) Effects of stretching on optical light transmittance of stretchable anodic PEDOT:PSS at different strain levels; (b-c) optical images of typical samples of the unstretched, stretched and over stretched stretchable PEDOT:PSS film. Reproduced from Oyewole, Oluwaseun, Oyewole, Deborah, Oyelade, Omolara, *et al.*, 2020. Failure of stretchable organic solar cells under monotonic and cyclic loading. Macromolecular Materials and Engineering 305 (11), 2000369, with the permission of Wiley Publishing.

strains are removed after few cycles. The optical absorbance of the emissive stretchable perovskite layer also decreased after cyclic deformation (**Fig. 14**(b)). The decrease in the absorbance is evident in the observed cracking and debonding of the layered structures (**Fig. 12**).

Effects of Fatigue Failure on Performance Characteristics

The effects of fatigue failure on performance characteristics of SOSCs have been demonstrated (Oyewole *et al.*, 2020). The lifetimes of the devices decrease with increasing strain range **Fig. 14**(c)). The decrease can be associated to the increasing initiation and propagation of cracks, as well as debonding of films, as the strain range increases. There is also an increase in the turn-on voltage of PeLED devices (**Fig. 14**(d)) which can be attributed to the observed cracking and debonding of the films. The PEO matrix of the PeLED structures can also stretched in a way that reduces the number of perovskite crystals within a region in the structures. This reduction in the number of perovskite crystals at a given region, can also make the devices to turn-on at higher bias voltage.

Summary and Concluding Remarks

This article presents the fatigue and fracture of FSE structures using a combination of analytical/computational and experimental technique. The critical conditions for deformation of FSE, that are necessary for the design of robust structures, are elucidated along with the stress-induced failure of FSE structures under 1D and 2D deformations. By using the understanding of the root cause failure of FSE structure during operating conditions, the designs of FSE have been shown to include wavy design, island-interconnect, fractal design and origami and kirigami structures. The design concept of fully stretchable electronic structures for applications in solar cells and light emitting devices have also been demonstrated using simple fabrication techniques.

The article then explored the fatigue testing techniques and analysis for layered thin film structures using typical stretchable organic solar cells and perovskite light emitting device structures. The fatigue lifetimes are predicted using a Coffin-Manson expression. The associated fatigue failures include cracking of films, interfacial cracking, delamination of film, delamination-induced buckling, wrinkling and debonding of thin films. The failures are used to elucidate the optoelectronic performance of the FSE structures.

In the case of stretchable organic solar cells, there are changes in the optoelectronic properties of the stretchable organic solar cells, under cyclic loading are associated with deformation and cracking phenomena, as well as interfacial cracks between the anodic PEDOT:PSS layers and the PDMS substrates. The fatigue lives of the flexible thin film SOSC structures are also shown to be

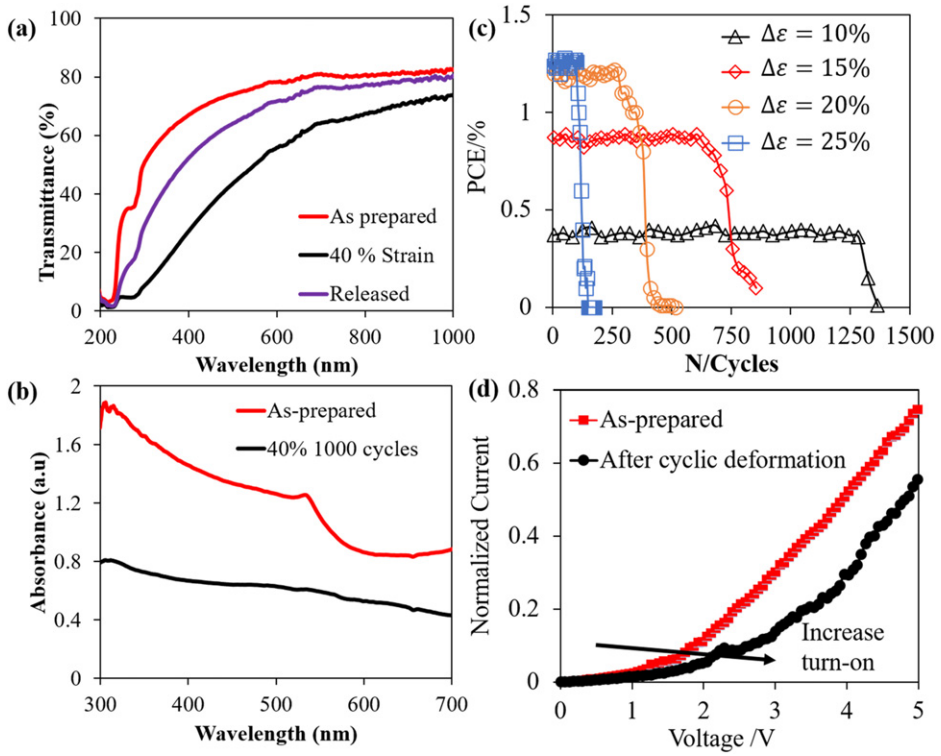

Fig. 14 Effects of Fatigue failure on optoelectronic properties of stretchable electronic structures: (a) effect of strains on transmittance of PEDOT:PSS + PEO-coated PDMS, (b) absorbance of cyclically deformed PeLED structure, (c) Effects of fatigue failure on power conversion efficiency of SOSC structure [Reprinted from Journal of Macromolecular Materials and Engineering, Wiley] and (d) Current-voltage of as-prepared and cyclically deformed PeLED structure.

well characterized by the Coffin-Manson model, while the failure phenomena observed during cyclic loading are shown to degrade the current-voltage characteristics and photoconversion efficiencies of the SOSCs, and the transmittance of the PEDOT:PSS anode. In the case of fully stretchable perovskite light emitting devices, the electrical properties are also influenced by cyclic loadings. The turn-on voltages of the PeLEDs are found to increase at 20% strain due increased number of cycles. The understanding of the fatigue behavior of FSE structures can be used for the design and manufacturing of flexible and stretchable electronic systems.

References

Agyei-Tuffour, B., Doumon, N.Y., Rwenyagila, E.R., *et al.*, 2017a. Pressure effects on interfacial surface contacts and performance of organic solar cells. Journal of Applied Physics 122 (20).

Agyei-Tuffour, B., Doumon, N.Y., Rwenyagila, E.R., *et al.*, 2017b. Pressure effects on interfacial surface contacts and performance of organic solar cells. Journal of Applied Physics 122 (20).

Akogwu, Onobu, Kwabi, David, Munhutu, Auxillia, Tong, Tiffany, Soboyejo, W.O., 2010. Adhesion and cyclic stretching of au thin film on poly(Dimethyl-Siloxane) for stretchable electronics. Journal of Applied Physics 108 (12).

Akogwu, Onobu, Kwabi, David, Midturi, Swaminadham, *et al.*, 2010. Large strain deformation and cracking of nano-scale gold films on PDMS substrate. Materials Science & Engineering B 170 (1–3), 32–40.

Akre, Karin L., Farris, Hamilton E., Lea, Amanda M., Page, Rachel A., Ryan, Michael J., 2011. Signal perception in frogs and bats and the evolution of mating signals. Science 333 (6043), 751–752.

Asare, J., Türköz, E., Agyei-Tuffour, B., *et al.*, 2017. Effects of pre-buckling on the bending of organic electronic structures. AIP Advances 7 (4).

Asare, Joseph, Agyei-Tuffour, B., Oyewole, O.K., Zebaze-Kana, G.M., Soboyejo, W.O., 2015. Deformation and failure of bendable organic solar cells. Advanced Materials Research 1132, 116–124.

Bade, Sri, Ganesh, R., Shan, Xin, *et al.*, 2017. Stretchable light-emitting diodes with organometal-halide-perovskite–polymer composite emitters. Advanced Materials 29 (23), 1607053.

Baran, Derya, Corzo, Daniel, Blazquez, Guillermo Tostado, 2020. Flexible electronics: Status, challenges and opportunities. Frontiers in Electronics 0, 2.

Bowden, N., Brittain, S., Evans, A.G., Hutchinson, J.W., Whitesides, G.M., 1998. Spontaneous formation of ordered structures in thin films of metals supported on an elastomeric polymer. Nature 393 (6681), 146–149.

Bowden, Ned, Wilhelm, T.S.Huck, Kateri, E.Paul, George, M.Whitesides, 1999. The controlled formation of ordered, sinusoidal structures by plasma oxidation of an elastomeric polymer. Applied Physics Letters 75 (17), 2557–2559.

Cao, Weiran, Zheng, Ying, Li, Zhifeng, Wrzesniewski, Edward, Hammond, William T., 2012. Flexible organic solar cells using an oxide / metal / oxide trilayer as transparent electrode. Organic Electronics 13 (11), 2221–2228.

Chattopadhyay, Soma, 2007. Biaxially stretchable 'wavy' silicon nanomembranes on elastomeric supports fabricated. MRS Bulletin 32 (8), 606.

Chen, X., Hutchinson, John W., 2004. Herringbone buckling patterns of compressed thin films on compliant substrates. Journal of Applied Mechanics, Transactions 71 (5), 597–603.

Cho, Yigil, Shin, Joong Ho, Costa, Avelino, *et al.*, 2014. Engineering the shape and structure of materials by fractal cut. Proceedings of the National Academy of Sciences of the United States of America 111 (49), 17390–17395.

Dennler, Gilles, Lungenschmied, C., Neugebauer, H., Sariciftci, N.S., Labouret, A., 2005. Flexible, conjugated polymer-fullerene-based bulk-heterojunction solar cells: basics, encapsulation, and integration. Journal of Materials Research 20 (12), 3224–3233.

Ebata, Yuri, Croll, Andrew B., Crosby, Alfred J., 2012. Wrinkling and strain localizations in polymer thin films. Soft Matter 8 (35), 9086–9091.

Evans, A.G., Hutchinson, J.W., 1995. The thermomechanical integrity of thin films and multilayers. Acta Metallurgica Et Materialia 43 (7), 2507–2530.

Fan, Jonathan A., Yeo, Woon-Hong, Su, Yewang, *et al.*, 2014. Fractal design concepts for stretchable electronics. Nature Communications 5 (1), 1–8.

Fei, Huiyang, Jiang, Hanqing, Khang, Dahl-Young, 2009. Nonsinusoidal buckling of thin gold films on elastomeric substrates. Journal of Vacuum Science & Technology A: Vacuum, Surfaces, and Films 27 (3), L9–L12.

Forrest, Stephen R., 2004. The path to ubiquitous and low-cost organic electronic appliances on plastic. Nature 428 (6986), 911–918.

Genzer, Jan, Groenewold, Jan, 2006. Soft matter with hard skin: From skin wrinkles to templating and material characterization. Soft Matter 2 (4), 310–323.

Green, Martin A., Anita, Ho-Baillie, Henry, J.Snaith, 2014. The emergence of perovskite solar cells. Nature Photonics 8 (7), 506–514.

Guo, Chuan, Fei, Tianyi, Sun, Qihan, *et al.*, 2014. Highly stretchable and transparent nanomesh electrodes made by grain boundary lithography. Nature Communications 5, 1–8.

Hanakata, Paul Z., Qi, Zenan, Campbell, David K., Harold, S.Park, 2016. Highly stretchable MoS2 kirigami. Nanoscale 8 (1), 458–463.

Heidari, Hadi, Wacker, Nicoleta, Dahiya, Ravinder, 2017. Bending induced electrical response variations in ultra-thin flexible chips and device modeling. Applied Physics Reviews 4 (3), 1–20.

Huang, R., Prévost, J.H., Huang, Z.Y., Suo, Z., 2003. Channel-cracking of thin films with the extended finite element method. Engineering Fracture Mechanics 70 (18), 2513–2526.

Huang, X., Zhao, Z., Cao, L., *et al.*, 2015. High-performance photovoltaic perovskite layers fabricated through intramolecular exchange. Science 348 (6240), 1230–1234.

Huang, Z.Y., Hong, W., Suo, Z., 2005. Nonlinear analyses of wrinkles in a film bonded to a compliant substrate. Journal of the Mechanics and Physics of Solids 53 (9), 2101–2118.

Jia, Zheng, Tucker, Matthew B., Li, Teng, 2011. Failure mechanics of organic-inorganic multilayer permeation barriers in flexible electronics. Composites Science and Technology 71 (3), 365–372.

Jiang, Hanqing, Khang, Dahl Young, Song, Jizhou, *et al.*, 2007. Finite deformation mechanics in buckled thin films on compliant supports. Proceedings of the National Academy of Sciences of the United States of America 104 (40), 15607–15612.

Kaltenbrunner, Martin, White, Matthew S., Głowacki, Eric D., *et al.*, 2012. Ultrathin and lightweight organic solar cells with high flexibility. Nature Communications 3.

Kan, Chi Wai, Lam, Yin Ling, 2021. Future trend in wearable electronics in the textile industry. Applied Sciences 11 (9).

Khang, Dahl, Rogers, Young, John A., Lee, Hong H., 2009. Mechanical buckling: Mechanics, metrology, and stretchable electronics. Advanced Functional Materials 19 (10), 1526–1536.

Kim, Dae Hyeong, Rogers, John A., 2008. Stretchable electronics: Materials strategies and devices. Advanced Materials 20 (24), 4887–4892.

Kim, Dae Hyeong, Song, Jizhou, Won, Mook Choi, *et al.*, 2008. Materials and Noncoplanar Mesh Designs for Integrated Circuits with Linear Elastic Responses to Extreme Mechanical Deformations. Proceedings of the National Academy of Sciences of the United States of America 105 (48), 18675–18680.

Kim, Dae-Hyeong, Xiao, Jianliang, Song, Jizhou, Huang, Yonggang, Rogers, John A., 2010. Stretchable, curvilinear electronics based on inorganic materials. Advanced Materials 22 (19), 2108–2124.

Kim, Hyun Min, Kim, Yun Cheol, An, Hee Ju, Myoung, Jae-Min, 2020. Highly stretchable and contact-responsive light-emitting diodes based on MAPbBr3–PEO composite film. Journal of Alloys and Compounds 819. 153360.

Kim, Mijung, Park, Jihun, Ji, Sangyoon, *et al.*, 2016. Fully-integrated, bezel-less transistor arrays using reversibly foldable interconnects and stretchable origami substrates. Nanoscale 8 (18), 9504–9510.

Kim, Tae-Wook, Lee, Jong-Sung, Kim, Young-Cheon, Joo, Young-Chang, Kim, Byoung-Joon, 2019. Bending strain and bending fatigue lifetime of flexible metal electrodes on polymer substrates. Materials 12 (15).

Kim, Yonghee, Young Kweon, O., Won, Yousang, Oh, Joon Hak, 2019. Deformable and stretchable electrodes for soft electronic devices. Macromolecular Research 27 (7), 625–639.

Ko, Heung Cho, Stoykovich, Mark P., Song, Jizhou, *et al.*, 2008. A hemispherical electronic eye camera based on compressible silicon optoelectronics. Nature 454 (7205), 748–753.

Kraft, O., Schwaiger, R., Wellner, P., 2001. Fatigue in thin films: Lifetime and damage formation. Materials Science and Engineering A 319–321, 919–923.

Lacour, Stephanie P., Jones, Joyelle, Wagner, Sigurd, Li, Teng, Zhigang, Suo, 2005. Stretchable interconnects for elastic electronic surfaces. Proceedings of the IEEE 93 (8), 1459–1467.

Lacour, Stéphanie P., Jones, Joyelle, Suo, Z., Wagner, Sigurd, 2004. Design and performance of thin metal film interconnects for skin-like electronic circuits. Electron Device Letters 25 (4), 179–181.

Lacour, Stéphanie P., Jones, Joyelle, Wagner, Sigurd, Li, Teng, Suo, Z., 2006. Elastomeric interconnects. International Journal of High Speed Electronics and Systems.

Lee, Jongho, Wu, Jian, Shi, Mingxing, *et al.*, 2011a. Stretchable GaAs photovoltaics with designs that enable high areal coverage. Advanced Materials 23 (8), 986–991.

Lee, Jongho, Wu, Jian, Shi, Mingxing, *et al.*, 2011b. Stretchable GaAs photovoltaics with designs that enable high areal coverage. Advanced Materials 23 (8), 986–991.

Li, Teng, Suo, Zhigang, Lacour, Stéphanie P., Wagner, Sigurd, 2005. Compliant thin film patterns of stiff materials as platforms for stretchable electronics. Journal of Materials Research.

Lim, Yein, Yoon, Jangyeol, Yun, Junyeong, *et al.*, 2014. Biaxially stretchable, integrated array of high performance microsupercapacitors. ACS Nano 8 (11), 11639–11650.

Lipomi, Darren J., Benjamin, C.K.Tee, Vosgueritchian, Michael, Bao, Zhenan, 2011. Stretchable organic solar cells. Advanced Materials 23 (15), 1771–1775.

Lipomi, Darren J., Jennifer A.Lee, Michael Vosgueritchian, Benjamin C.K. Tee, John A. Bolander, and Zhenan Bao. 2012. "Electronic Properties of Transparent Conductive Films of PEDOT:PSS on Stretchable Substrates." Chemistry of Materials 24 (2), 373-382.

Liu, Wei, Min Sang Song, Biao Kong, and Yi Cui. 2017. "Flexible and Stretchable Energy Storage: Recent Advances and Future Perspectives." Advanced Materials 29 (1), 1603436.

Liu, Yuhao, Pharr, Matt, Salvatore, Giovanni Antonio, 2017. Lab-on-skin: A review of flexible and stretchable electronics for wearable health monitoring. ACS Nano 11 (10), 9614–9635.

Liu, Yuqiang, Qi, Ning, Song, Tao, *et al.*, 2014. Highly flexible and lightweight organic solar cells on biocompatible silk fibroin. ACS Applied Materials and Interfaces 6 (23), 20670–20675.

Logothetidis, Stergios. 2008. Flexible organic electronic devices : Materials , process and applications." 152, 96–104.

Ma, Qiang, Zhang, Yihui, 2016. Mechanics of fractal-inspired horseshoe microstructures for applications in stretchable electronics. Journal of Applied Mechanics, Transactions 83 (11), 1–19.

Mao, Youdong, Wang, Wei L., Wei, Dongguang, Kaxiras, Efthimios, Sodroski, Joseph G., 2011. Graphene structures at an extreme degree of buckling. ACS Nano 5 (2), 1395–1400.

Mei, Haixia, Rui Huang. 2013. Wrinkling and delamination of thin films on compliant substrates. In: Proceedings of the 13th International Conference on Fracture 2013, ICF 2013.
Miao, Feng, Strachan, John Paul, Yang, J.Joshua, *et al.*, 2011. Anatomy of a nanoscale conduction channel reveals the mechanism of a high-performance memristor. Advanced Materials 23 (47), 5633–5640.
Midturi, Swaminadham, 2010. Stress-strain behavior of nano / micro thin film materials. ARPN Journal of Engineering and Applied Sciences 5 (3), 72–76.
Momodu, D.Y., Tong, T., Zebaze Kana, M.G., Chioh, A.V., Soboyejo, W.O., 2014. Adhesion and degradation of organic and hybrid organic-inorganic light-emitting devices. Journal of Applied Physics 115 (8).
Nogi, Masaya, Komoda, Natsuki, Otsuka, Kanji, Suganuma, Katsuaki, 2013. Foldable nanopaper antennas for origami electronics. Nanoscale 5 (10), 4395–4399.
Nolte, Adam J., Jun Young Chung, Chelsea S., Davis, Christopher, M.Stafford, 2017. Wrinkling-to-delamination transition in thin polymer films on compliant substrates. Soft Matter 13 (43), 7930–7937.
Oyewole, O.K., Oyewole, D.O., Asare, J., *et al.*, 2015c. Failure mechanisms in layers relevant to stretchable organic solar cells. Advanced Materials Research 1132, 106–115.
Oyewole, O.K., Asare, J., Oyewole, D.O., *et al.*, 2015b. Effects of adhesion and stretching on failure mechanisms and optical properties of organic solar cells. Advanced Materials Research 1132, 89–105.
Oyewole, O.K., Yu, D., Du, J., *et al.*, 2015d. Lamination of organic solar cells and organic light emitting devices: Models and experiments. Journal of Applied Physics 118 (7).
Oyewole, O.K., Yu, D., Du, J., *et al.*, 2015a. Micro-wrinkling and delamination-induced buckling of stretchable electronic structures. Journal of Applied Physics 117 (23).
Oyewole, Oluwaseun, Deborah, Oyewole, Omolara, Oyelade, *et al.*, 2020. Failure of stretchable organic solar cells under monotonic and cyclic loading. Macromolecular Materials and Engineering 305 (11), 2000369.
Oyewole, Oluwaseun K., 2015. Effects of Adhesion and Deformation on Stretchable Electronic Structures. African University of Science and Technology.
Qi, Zenan, David, K.Campbell, Park, Harold S., 2014. Atomistic simulations of tension-induced large deformation and stretchability in graphene kirigami. Physical Review B - Condensed Matter and Materials Physics 90 (24), 1–7.
Saleh, Rafat, Maximilian, Barth, Wolfgang, Eberhardt, André, Zimmermann, 2021. Bending setups for reliability investigation of flexible electronics. Micromachines 12 (1), 1–22.
Sekitani, Tsuyoshi, Noguchi, Yoshiaki, Hata, Kenji, *et al.*, 2008. A rubberlike stretchable active matrix using elastic conductors. Science 321 (5895), 1468–1472.
Sekitani, Tsuyoshi, Nakajima, Hiroyoshi, Maeda, Hiroki, *et al.*, 2009. Stretchable active-matrix organic light-emitting diode display using printable elastic conductors. Nature Materials 8 (6), 494–499.
Shyu, Terry C., Pablo F. Damasceno, Paul M. Dodd, Aaron Lamoureux, Lizhi Xu, Matthew Shlian, Max Shtein, Sharon C. Glotzer, and Nicholas A. Kotov. 2015. "A Kirigami Approach to Engineering Elasticity in Nanocomposites through Patterned Defects."
Someya, Takao, Sekitani, Tsuyoshi, 2009. Procedia chemistry. PROCHE 1 (1), 9–12.
Song, J., Jiang, H., Choi, W.M., *et al.*, 2008a. An analytical study of two-dimensional buckling of thin films on compliant substrates. Journal of Applied Physics 103 (1), 1–10.
Song, J., Jiang, H., Liu, Z.J., *et al.*, 2008b. Buckling of a stiff thin film on a compliant substrate in large deformation. International Journal of Solids and Structures 45 (10), 3107–3121.
Song, Zeming, Wang, Xu, Lv, Cheng, *et al.*, 2015. Kirigami-based stretchable lithium-ion batteries. Scientific Reports 5, 1–9.
Stafford, Christopher M., Bryan, D.Vogt, Harrison, Christopher, Julthongpiput, Duangrut, Huang, Rui, 2006. Elastic moduli of ultrathin amorphous polymer films. Macromolecules 39 (15), 5095–5099.
Stafford, Christopher M., Harrison, Christopher, Beers, Kathryn L., *et al.*, 2004. A buckling-based metrology for measuring the elastic moduli of polymeric thin films. Nature Materials 3, 545–550.
Su, Yewang, Liu, Zhuangjian, Kim, Seok, *et al.*, 2012. Mechanics of stretchable electronics with high fill factors. International Journal of Solids and Structures 49 (23–24), 3416–3421.
Su, Yewang, Wang, Shuodao, An Huang, Yong, *et al.*, 2015. Elasticity of fractal inspired interconnects. Small 11 (3), 367–373.
Suarez, Francisco, Parekh, Dishit P., Ladd, Collin, *et al.*, 2017. Flexible thermoelectric generator using bulk legs and liquid metal interconnects for wearable electronics. Applied Energy 202, 736–745.
Sun, Yugang, Rogers, John A., 2007. Inorganic semiconductors for flexible electronics. Advanced Materials 19 (15), 1897–1916.
Suo, Z., Prévost, J.H., Liang, J., 2003. Kinetics of crack initiation and growth in organic-containing integrated structures. Journal of the Mechanics and Physics of Solids 51 (11–12), 2169–2190.
Suresh, S., 1999. Fatigue of Materials. Cambridge University Press,. pp. 137–139.
Tong, T., Babatope, B., Admassie, S., *et al.*, 2009. Adhesion in organic electronic structures. Journal of Applied Physics 106 (8).
Toth, F., Rammerstorfer, F.G., Cordill, M.J., Fischer, F.D., 2013. Detailed modelling of delamination buckling of thin films under global tension. Acta Materialia 61 (7), 2425–2433.
Tucker, Matthew B., Hines, D.R., Li, Teng, 2009. A quality map of transfer printing. Journal of Applied Physics 106 (10), 103504.
Wang, Bo, Bao, Siyuan, Vinnikova, Sandra, Ghanta, Pravarsha, Wang, Shuodao, 2017. Buckling analysis in stretchable electronics. npj Flexible Electronics 1 (1), 1–9.
Watanabe, Masashi, 2012. Wrinkles with a well-ordered checkerboard pattern, created using dip-coating of poly(methyl methacrylate) on a UV-ozone-treated poly (dimethylsiloxane) substrate. Soft Matter 8, 1563–1569.
Watanabe, Masashi, Shirai, Hirofusa, Hirai, Toshihiro, 2002. Wrinkled polypyrrole electrode for electroactive polymer actuators. Journal of Applied Physics 92 (8), 4631–4637.
Webb, R.Chad, Bonifas, Andrew P., Behnaz, Alex, *et al.*, 2013. Ultrathin conformal devices for precise and continuous thermal characterization of human skin. Nature Materials 12 (10), 938–944.
Wu, Dan, Xie, Huimin, Yin, Yajun, Tang, Minjin, 2013. Micro-scale delaminating and buckling of thin film on soft substrate. Journal of Micromechanics and Microengineering 23 (3).
Wu, Wei, 2019. Stretchable electronics: Functional materials, fabrication strategies and applications. Science and Technology of Advanced Materials.
Xu, Sheng, Zhang, Yihui, Cho, Jiung, *et al.*, 2013. Stretchable batteries with self-similar serpentine interconnects and integrated wireless recharging systems. Nature Communications 4.
Yi, Seol-Min, Choi, In-Suk, Kim, Byoung-Joon, Joo, Young-Chang, 2018. Reliability issues and solutions in flexible electronics under mechanical fatigue. Electronic Materials Letters 14 (4), 387–404.
Yoo, P.J., Suh, K.Y., Park, S.Y., Lee, H.H., 2002. Physical self-assembly of microstructures by anisotropic buckling. Advanced Materials 14 (19), 1383–1387.
Yu, D., Oyewole, O.K., Kwabi, D., *et al.*, 2014a. Adhesion in flexible organic and hybrid organic/inorganic light emitting device and solar cells. Journal of Applied Physics 116 (7).
Yu, D., Oyewole, O.K., Kwabi, D., *et al.*, 2014b. Adhesion in flexible organic and hybrid organic/inorganic light emitting device and solar cells. Journal of Applied Physics 116 (7).
Zhang, Yihui, Xu, Sheng, Fu, Haoran, *et al.*, 2013. Buckling in serpentine microstructures and applications in elastomer-supported ultra-stretchable electronics with high areal coverage. Soft Matter 9, 8062–8070.